2007

EXPERIMENTAL INVESTIGATION OF PCD COMPACT CORE DRILL PERFORMANCE ON BASALT SIMULATING SUSTAINABLE DRY DRILLING ON MARS

Sandeep Manthri
University of Kentucky, spmant2@uky.edu

ABSTRACT OF THESIS

EXPERIMENTAL INVESTIGATION OF PCD COMPACT CORE DRILL PERFORMANCE ON BASALT SIMULATING SUSTAINABLE DRY DRILLING ON MARS

Missions to Mars aim to characterize rock and subsurface soil samples and possibly bring some back to Earth for more thorough and sophisticated examination. The Martian surface is covered with basalt which has high compressive strength (>130 MPa), and is more difficult to drill than the much softer sedimentary formations that are presently being drilled using diamond core drills.

The main objective of this thesis work is to provide the requisite groundwork towards the development of improved and sustainable drills for subsurface drilling applications on Mars, when their goals are obtaining samples. Since progressive drill-wear is substantial in sustained drilling, the experiments were designed and conducted to study the tool-wear mechanisms and understand the associated effects on drilling performance in subsurface drilling of basalt. Core drilling experiments are conducted with different drill geometries and cutting conditions in a Martian simulant, basaltic rock; monitoring thrust force, torque and measuring tool-wear for a series of successive depth-increments. Based on the experimental results an optimization model has been developed for maximizing drilling depth with minimum tool-wear. This preliminary work will help the development of smart and sustainable drills for dry drilling applications for future NASA missions to Mars.

Keywords: Core drilling, PCD compact, Basalt, Sustainable dry drilling, Mars

Sandeep Manthri

Date: 11/06/2007

EXPERIMENTAL INVESTIGATION OF PCD COMPACT CORE DRILL PERFORMANCE ON BASALT SIMULATING SUSTAINABLE DRY DRILLING ON MARS

By

Sandeep Manthri

Dr. I.S. Jawahir

(Director of Thesis)

Dr. D.P. Sekulic

(Director of Graduate Studies)

Date: 11/06/2007

RULES FOR THE USE OF THE THESIS

Unpublished theses submitted for the Master's degree and deposited in the University of Kentucky Library are as a rule open for inspection, but are to be used only with due regard to the rights of the authors. Bibliographical references may be noted, but quotations or summaries of parts may be published only with the permission of the author, and with the usual scholarly acknowledgements.

Extensive copying or publication of the thesis in whole or in part also requires the consent of the Dean of the Graduate School of the University of Kentucky.

A library that borrows this thesis for use by its patrons is expected to secure the signature of each user.

Name	Date

THESIS

Sandeep Manthri

The Graduate School

University of Kentucky

2007

EXPERIMENTAL INVESTIGATION OF PCD COMPACT CORE DRILL PERFORMANCE ON BASALT SIMULATING SUSTAINABLE DRY DRILLING ON MARS

THESIS

A thesis submitted in partial fulfillment of the requirements
for the degree of Master of Science in the
College of Engineering at the
University of Kentucky

By

Sandeep Manthri

Lexington, Kentucky

Director: Dr. I.S. Jawahir, Professor of Mechanical Engineering

Lexington, Kentucky

2007

MASTER'S THESIS RELEASE

I authorize the University of Kentucky

Libraries to reproduce this thesis in

whole or in part for the purpose of research.

SIGNED: SANDEEP MANTHRI

DATE: 11/06/2007

Dedicated to,

My Family and Friends

ACKNOWLEDGEMENTS

I take this opportunity to thank several people who guided me during the advancement of my research work. I would like to express my sincere gratitude to Dr. I.S. Jawahir for ongoing financial support, allowing me to work in this innovative project and appreciate the disciplinary guidance provided by him at every juncture of my thesis. My special thanks to Dr. O.W. Dillon Jr. for his valuable ideas and feedback to help me resolve critical problems faced during the research. I would also thank Dr. K.E. Rouch for sparing valuable time to serve on the examination committee.

I am grateful to our technical staff, Bill Young and my colleagues, Franci Pusavec, Ashish Deshpande and Shi Chen for their timely assistance and advices throughout my work while I have always enjoyed working with them. I thank Dr. K.A. Zacny, Honeybee Robotics for providing us with the core drill and PCD compact inserts, Dr. P.W. Weiblen, University of Minnesota for supplying the Duluth basalt rocks which were used in the experiments and Dr. L.A. Taylor for his valuable suggestions throughout this project.

Acknowledgements to the Center for Manufacturing staff for their cooperation in the administrative tasks performed during the course of project completion. I especially thank Dr. Hui Zhao for providing me with the necessary training to use the optical microscope that helped me obtain good results in the project.

Finally, I would like to thank my parents, family, friends and my adorable cousin Uma for providing the necessary support during my research.

TABLE OF CONTENTS

LIST OF TABLES

LIST OF FIGURES

LIST OF FILES

1. Thesis.pdf – 2.6 Mb (Maximum file size)

CHAPTER 1

INTRODUCTION

1.1 Introduction

Planetary exploration missions aim to obtain samples and possibly return them to Earth for more thorough examination. In particular missions to Mars with such capabilities are contemplated in the near future and there is a strong interest in obtaining a specimen from the sub-surface of Mars. This is a study of drill parameters and geometry influence on tool-life based on the core drilling experimental results in Martian simulant rock, basalt.

1.1.1 Martian Environment

The surface temperature on Mars is typically in the region of -100° C while the atmospheric pressure ranges from 1-11 torr (0.001 – 0.015 atmosphere). The low temperatures on Mars preclude the use of many materials such as metals with a body centered cubic structure (eg. Ferritic steels), as they become brittle at low temperature. The low pressure will also reduce the heat transfer by convection (Zacny and Cooper, 2005). The geology of the surface of Mars is still incompletely understood.

1.1.2 Diamond Drills

The drill bit to be used for Martian drilling must have the ability to penetrate a variety of formations such as frozen mud, ice, sedimentary rocks and igneous rocks. The drills tested so far for potential Martian drilling can be categorized into diamond impregnated core drills and polycrystalline diamond (PCD) compact core bits. The types of rocks to be

drilled using the core drills are sedimentary rocks such as sandstone, limestone, travertine etc. (Magnani et al., 2004; Zacny and Cooper, 2004). However, much of the Martian surface is basalt; the sedimentary formations are expected to be much softer and therefore much easier to penetrate than basalt. The high compressive strength of basalt (>130 MPa) poses a challenge when designing a drill bit suitable for remote drilling on Mars (Grady, 1999). The large variation in basalt strength is also a consideration. Even so, diamond tools have been successful in drilling hard rocks such as granite, marble etc. on Earth whose compressive strengths are in similar range to that of basalt.

1.1.3 Rock Drilling

In rotary drilling, when a drilling tool hits the rock, the material is forced to crack because of two actions, a compressive vertical force and horizontal action for chip separation by rotation. Thus monitoring thrust force and torque can provide useful information on drill bit wear during the drilling process.

In rotary drilling, the rock material is removed in the form of fine powder. Conventional drilling on Earth uses either a liquid or air for flushing the rock cuttings from the hole. But the Martian atmosphere and NASA's planetary protection policy to avoid the biological contamination of other solar system bodies such as Mars (Planetary Protection Policy), precludes the use of liquids for cuttings removal; the drilling machines utilize mechanical means of cuttings removal such as an auger. However, an auger can substantially contribute to the total power requirements, and in the worst case can cease to drill. Experiments conducted under Martian pressures showed that intermittent blasts

of gas at low differential pressures can effectively lift the cuttings out of the hole (Zacny et al., 2005).

1.2 Overview of Thesis

The main objective of this thesis work is to provide the groundwork towards the development of improved and sustainable drills for subsurface dry drilling applications on Mars, with the goal of obtaining samples of basalt rock suitable for further analysis. It involves experimentation with different drill geometries, drill materials and cutting conditions when cutting basalt rock. Since the progressive drill-wear would be expected to be substantial in dry drilling on Mars, the experiments are designed to study the tool-wear mechanisms and to understand the associated effects of drilling performance due to changing drill edge conditions in subsurface drilling on a Martian-like material, basalt. The long range thesis objective is to optimize the drill geometry to enhance the performance especially when drilling basalt.

Chapter 2 describes the summary of the relevant prior research in Martian drilling by different space agencies. The tool-wear behavior of diamond core drills viz. PCD compact core drills and diamond impregnated core drill are discussed.

Chapter 3 covers the details related to the present experimental setup, the properties of the basalt rock, discussion of preliminary experimental results followed by design of experiments and finally the experimental procedure itself.

Chapter 4 describes the analysis of experimental results and optimization of cutting conditions and drill geometry based on the data consisting of thrust force, torque and tool-wear of the PCD compact core drill.

Chapter 5 lists the conclusions of this project and describes the performance of PCD compact core drills when cutting basalt rock in this experimental investigation and the relevance of the current research with regards to future Martian drilling.

CHAPTER 2

REVIEW OF PRIOR RESEARCH WORK ON MARTIAN DRILLING

International companies and organizations have designed prototypes and engineering test models for Martian drilling purposes. In the future, the European Space Agency (ESA) and NASA have preliminary plans to send a Rover, which could perform up to 2 meter deep drilling and sampling of Martian Regolith. The required thrust force for drilling application is presumed to be provided by a Lander/Rover on which the core drill bit is assembled. ESA's ExoMars Rover has a planned mass of 220 Kg and NASA's MSL Rover/platform more than 100 kg, possibly even 600 kg (Anttila and Ylikorpi, 2003).

2.1 Drilling on Mars

Space craft lands on Martian surface, lander deploys Rover, and Rover uses a drill to extract samples. Anomalies that may occur while drilling can be sticking in the hole and/or damaged drill bits etc. The drilling system should be able to penetrate and sample the Martian ground up to 2 meters, going into an unknown material whose hardness is up to number 8 on the Mohs' scale. It has been learned from the NASA Viking and Pathfinder missions, sampling of surface soil and rocks can gain only limited scientific information (Anttila et al., 2002).

The choice of drilling equipment will depend on many inter-related factors, but it is clear that it is more important for the drill to be able to make progress in any and all terrain than to be able to drill rapidly in a specific formation. Therefore drill bits such as

diamond impregnated segments or polycrystalline diamond compact (PCD) bits have been tested on existing drilling equipment.

2.2 Diamond-impregnated Drill Bits

A diamond-impregnated bit may be the most probable choice for Mars drilling applications because it can be used to drill the hard rocks, including the most common rocks on Mars i.e., basalt and andesite. In addition to volcanic rocks, the bit might also have to drill through other geological formations such as clay-rich soils. This argument supposes that the Martian drill system will not have an option for changing bits.

Zacny and Cooper (2004) have used a 44 mm diameter diamond-impregnated core bit to drill Ohio sandstone rock specimen of specific gravity 2.06, porosity 20% and compressive strength 48 MPa. The rock specimen is water saturated up to 60% and placed in the freezer at -80° C which increases compressive strength of rock by 50% (Zacny and Cooper, 2006). The rate of penetration varied between 30 cm/hr to 36 cm/hr. The drill bit temperature reached 60° C when starting at 24° when it drilled into a rock specimen (which is at -60° C) for 2040 seconds. The acquired drilling data included thrust force, rotational speed of the drill, and reaction torque from the rock on the drill bit.

The drill bit used by Zacny and Cooper (2004) consists of diamond-impregnated cutting segments, selected for dry drilling in sandstone (soft rock since its compressive strength is 48 MPa). The most abundant element found in the cutting segment is cobalt (Co)

followed by iron (Fe) and nickel (Ni) as determined from using Scanning Electron Microscopy coupled with Energy Dispersive X-ray Spectrometry. The matrix made of tungsten is more highly abrasive resistant than a matrix made of Co, Fe and Ni which is more abrasive resistant than copper and bronze alloys. The design of diamond-impregnated drill bits is based on the idea that the wear of the matrix should be matched with the wear of the diamonds. If the matrix is made too hard, diamonds can be worn down to the extent that they no longer cut. The result is that the bit stops drilling. On the other hand if the matrix is made too soft, the tool life would be small. It is very difficult to optimize the matrix properties of a diamond without prior knowledge of the properties of the material in which the bit will be drilling (Zacny and Cooper, 2004).

2.3 Hard Alloy Core Drill

Micro Robots for Scientific Applications 2 (MRoSA2) drilling system consists of a roving platform and Drilling and Sampling Subsystem (DSS) weighing, 11 Kg. The DSS designed and manufactured for MRoSA2 weighs 5 Kg. During drilling, a core develops inside the drill, while the bit crown chips the material chips are conveyed to the surface by the external helical profile of the drill. A 16 mm diameter custom made alloy core drill (teratrio) optimizing at 27 N thrust force, 120 rpm, feed 2.2 mm/h drilled a 2.3 mm hole in granite in 1.3 hrs (Anttilla and Ylikorpi, 2003). The tool is designed to drill a 17 mm diameter hole to contain a 9 mm diameter and 15 mm long sample core. The tool bits have sharp cutting edges and are made of a hard alloy, hence limited to softer materials like limestone (Anttila et al., 2002). A Mafurite sample was collected after drilling for 162 min for a depth of 0.1 cm at 0.04 cm/hr.

2.4 Polycrystalline Diamond (PCD) Compact Bits

Cutters consisting of a layer of polycrystalline diamonds integrally bonded to a carbide substrate have been widely accepted for use on bits for the petroleum industry and for other drilling applications. The cutter segments are made of cemented tungsten carbide provided with a layer of polycrystalline diamond on the forward edge of the cutter. These bits are generally much more aggressive than diamond-impregnated bits and give higher rates of penetration (Zacny and Cooper, 2006).

Magnani et al. (2004) designed a complex rotary tool called DeeDri, shown in Figure 2.1 devoted to soil perforation and sample collection of Martian zone made of rocks similar to the terrestrial basalt. Radially mounted cutting bits are made of polycrystalline blades which are devoted to cut and remove rock chips. The diameter of the possible hole is 35 mm and core sample dimensions being 14 mm diameter and 25 mm length. The drilling and sample collections tests were carried into several materials: sand, gas concrete, tuff and travertine.

Figure 2.1: DeeDri PCD compact core drill along with sampling mechanism developed by the Italian space agency (Magnani et al., 2004)

Zacny and Cooper (2002) carried out comparative wear tests on polycrystalline diamond and tungsten carbide (WC) cutters, by machining granite rock cylinders on an instrumented lathe. It was observed that the polycrystalline diamond compact cutter removed 13 times more granite than WC before wearing out.

A major reason for ductility in the Martian surface is that it may contain water in the subsurface soils. In an experiment conducted to collect mud core samples under Martian atmospheric conditions the frozen mud was cut by the leading edge of the cutting segment and not by the surface diamonds. The water-saturated frozen soils tend to be ductile at few degrees below 0° C and require chisel type drill. Zacny and Cooper (2005) indicated that polycrystalline diamond compact type bit would be best choice while drilling frozen mud.

Zacny et al. (2006) tested two designs of drill bits, one with tungsten carbide (WC) cutters and other with polycrystalline diamond (PCD) compact cutters. PCD compact cutters were placed at negative rake angle of 15° and tested in lunar simulant prepared in laboratory whose compressive strength is 40 MPa. The comparison of the performance in terms of specific energy (energy required to drill a volume of rock) of the two cutters showed that PCD compact is more efficient than tungsten carbide bits in terrestrial applications. The specific energy required for PCD compact bit is 150 MJ/m^3 whereas WC bit needed 200 MJ/m^3.

Ersoy and Waller (1997) performed comparative experiments using PCD compact and impregnated diamond core bit on sandstone. The operating parameters to evaluate the drilling performance of both drills were rate of penetration, weight on bit (thrust force), rpm and torque. The tool-wear results measured in terms of bit weight loss showed that performance of PCD compact bits were better than diamond impregnated bits under similar conditions.

In recent publication, Zacny and Cooper (2007) tested the performance of PCD compact cutters on basalt rock with maximum thrust force of 950 N and 100 W drilling power. The flank wear recorded in their investigation was 0.2 mm after drilling 150 mm in the basalt rock. Hence, PCD compact core drills have been successful in drilling igneous rocks such as basalt.

2.5 Tool-wear Mechanism in PCD Compact Bit

In this section, the parameters that influence the tool-wear in PCD compact bits while drilling different rock formations encountered in oil-hole drilling and mining applications will be discussed. The published research on PCD compact tool-wear relevant to extra-terrestrial applications has been limited at the time of writing this thesis.

The factors that influence tool-wear in PCD compact tools during rock cutting can be broadly categorized as follows:

a) Cutting forces
b) Temperature of the cutting tool
c) Operating parameters such as cutting speed, feed and depth of cut
d) Geometry parameters such as rake angle, bit radius
e) Properties of the rock material

The visible effect of tool-wear in PCD compact tools is the growth of flank wear (also called wear flat) and its effect on cutting performance of PCD compact insert is shown by an increase in cutting forces and tool temperature. Checkina et al. (1996) developed a wear model to study the influence of diamond tool-wear on the rock cutting process. Lin et al. (1991) studied different modes of wear and failure mechanisms of PCD compact bits and found that the cutter force necessary to maintain a given depth of cut in a rock is proportional to the area of the flank wear.

Wilson and Vorono (2003) conducted experiments using a PCD compact tool on granite rock in which cutting forces are sampled at 1 sec intervals and forces were plotted using moving 10 sec average (since there has been considerable amount of fluctuation in force readings). The experimental results showed a rapid increase in normal force at 1200 – 1400 N and tool temperature at 500° C for a PCD compact cutter. Appl et al. (1993) performed a series of experiments to understand the effects of tool temperature and cutting forces on tool life of PCD compact bit while turning a granite rock cylinder. They found that the rate of tool-wear abruptly increased, by a factor of 50, when the measured PCD compact bit temperature exceeded 500° C. Glowka (1985) developed an abrasive wear model by experimenting with PCD compact cutters in four types of rocks. He demonstrated the significance of cutter forces and temperature in estimating the tool-wear. In his investigation thermally accelerated wear for a PCD compact tool occurred above 350° C.

Kolle (1996) conducted rock cutting experiments on five different rocks with varying strength and porosity using thermally stable diamond cutters mounted at a rake angle of negative 20°. The cutter wear was found to be minimum at high rotary speed in all the rock types. Glowka (1985) suggested that, in order to increase the tool life for PCD compact cutters in hard rock formations, the ratio of feed to speed should be maximized.

Wise et al. (2005) conducted a study focused on determining the consequences of changes in diamond thickness, diamond substrate and geometry parameter chamfer angle when drilling with a PCD compact insert in Sierra white granite. The rake angle selected in these experiments is negative 20° and the results of their investigation showed that the

variation in design and processing parameters strongly influenced drilling performance of PCD compact cutters when cutting hard rock formations. PCD compact bits with larger negative rake angle were recommended for drilling in hard and inhomogeneous rocks (Lin et al., 1991).

The rate of tool-wear in PCD compact cutters depends on the rock properties, such as compressive strength and porosity. The compressive strength of the rock is approximately equal to the normal stress on a PCD compact insert measured during cutting process (Appl et al., 1993;Zacny and Cooper, 2007). The porosity of the rock has an influence on the measurement of cutting forces especially in rotary core drilling process since the evacuation of rock particles is a big challenge in the absence of a coolant.

Lei and Kaitkay (2002) modeled a two dimensional rock cutting process studying the rock deformation process under various machining conditions in a Carthage limestone and explained that the large fluctuation in measured cutting forces is due to random breakage of contact bonds between rock particles. In a discrete element modeling of rotary rock drilling, Stavropoulou (2006) explained that cutting forces will fluctuate during the rock cutting cycle due to non-homogeneous nature of rock particles.

Apart from rotary drilling, Ultrasonic/sonic driller/corer, also called USDC, is another drilling mechanism tested for in-situ astrobiological exploration. USDC requires low axial force and power and has been successfully demonstrated when drilling ice, granite, diorite, basalt and limestone. The depth of the drilled hole in igneous basalt rock using

USDC is 25 mm in a time period of 2 hrs. The core sampling mechanism using ultrasonic technology is currently in design and modeling phase (Bar-Cohen et al., 2003).

From the above study, it has been noted that polycrystalline diamond bits have potential to perform better on Martian surface with variable terrain that potentially includes basalt rock. Most of the empirical and analytical models on PCD compact tool-wear are developed for improving the performance of the PCD compact tools during terrestrial drilling. Thus, an attempt is made in this thesis to experimentally investigate the drilling performance of PCD compact tools on Martian simulant, basalt, by minimizing the tool-wear while optimizing the cutting parameters involved in rock drilling.

CHAPTER 3

EXPERIMENTAL SET-UP AND PROCEDURE

This chapter describes the properties of the basalt rock, cutting tool-wear and procedure employed for conducting the experimental drilling work. The experimental set-up and the equipment used to control and monitor the involved parameters are explained in separate sections. A brief step by step procedure of how the experiments are planned and implemented is given; along with the discussion of certain preliminary results, obtained during core drilling in basalt.

3.1 Properties of Basalt Rock

Basalt is a type of igneous rock, extremely hard and having high abrasive resistance which is generally used as building stone in its natural form. It is expected to be one of the harder materials. Its hardness values range from 5 – 9 on Mohs' scale (Sheldon, 1977). The visible/near infra-red spectroscopic observations suggest that the Martian surface is dominated by basaltic formations (Wyatt and McSween Jr., 2002) and hence the core drill is likely to encounter basalt on planet Mars. Hence, by optimizing the drill geometry for cutting conditions for the hardest rock material, basalt, it is assumed that the drill bit could easily penetrate softer formations such as sedimentary rocks, mud, etc.

Rocks are generally characterized by properties such as porosity, specific gravity, thermal conductivity etc. but uniaxial compressive strength is considered as the basic property denoting the strength of a rock (Stavropoulou, 2006). The most common properties of a

basalt rock sample are shown in Table 3.1 (Grady, 1999; Glindermann et al., 2005). However, rocks are also inhomogeneous materials and contain cracks, thus there is a wide variation in their properties, including their compressive strength.

Table 3.1: Typical properties of common basalt rock

Property	**Value**
Compressive strength	130 MPa
Abrasivity	Class 3 (Highly abrasive)
Hardness	65 (HRF) ~ 6 (Mohs' scale)

In the current experiments, a basalt rock is obtained from a quarry situated in Duluth, Minnesota, United States of America (Courtesy: Dr. P.W. Weiblen). Two rock samples, designated as Rock 1 and Rock 2, which are identical in shape and approximate dimension 125 x 125 x 125 mm^3, are used to conduct the core drilling experiments. The properties of the basalt rock samples used in our experimental work are given in Table 3.2. The compressive strength of basalt rock can be approximately determined using thrust force and flank wear data that is presented in Appendix I based upon the equation developed by Zacny and Cooper (2007). Since the Mohs' scale indicates relative mineral hardness, the hardness of basalt rocks is determined here in by standard Rockwell testing equipment using a 1/16" steel ball indenter at load of 60 kgs. Density is obtained by actually measuring the mass and volume of cylindrical shaped basalt core samples.

Table 3.2: Measured properties of Duluth basalt rock used in experiments

Property	**Rock 1**	**Rock 2**
Compressive strength	448 ± 25 MPa	667 ± 31 MPa
Hardness	82 ± 5 (HRF) ~ 2.5 (Mohs' scale)	118 ± 8 (HRF) ~ 5.5 (Mohs' scale)
Density	2.23 gm/cc	2.39 gm/cc

3.2 Description of Core Drill

From the literature study and considering the core drills tested so far, for extraterrestrial applications the diamond impregnated bit becomes a good choice for highly igneous basalt rock. Certain disadvantages related to matrix properties and tool-wear has been identified among diamond impregnated bits with respect to drilling applications on Mars. The normal selection of matrix composition in diamond impregnated bits is completely dependent on the type of the rock to be drilled, i.e., the matrix selected to drill basalt rock may not be suitable for other types of rocks. The tool-wear on diamond impregnated bits is difficult to interpret and quantify since the tool-wear is not progressive. The methods employed so far in measuring tool-wear of diamond impregnated drills are determined by finding the weight and volume of the bit. Moreover it is difficult to design an optimum diamond impregnated bit by varying the geometry to drill on geologically uncertain surfaces such as those on Mars.

The core drill used for the reported experimentation is a Polycrystalline Diamond (PCD) compact core drill shown in Figure 3.1 with an outer diameter 38 mm and inner diameter 25 mm. It has 4 PCD compact inserts (Insert grade: CTH, supplied by Diamond abrasives corp., New York, USA) as shown and mounted at -10° rake angle with the support of

removable wedges. The dimensions of each insert are 6.0 x 3.5 x 1.6 mm and the average size of the diamonds is 25 microns. The thickness of the diamond layer is approximately 0.5 mm. PCD compact inserts are manufactured by sintering together carefully selected synthetic diamond particles at very high temperature and pressure in a solvent/catalyst metal. The orthogonal view of a single PCD insert is shown in Figure 3.2.

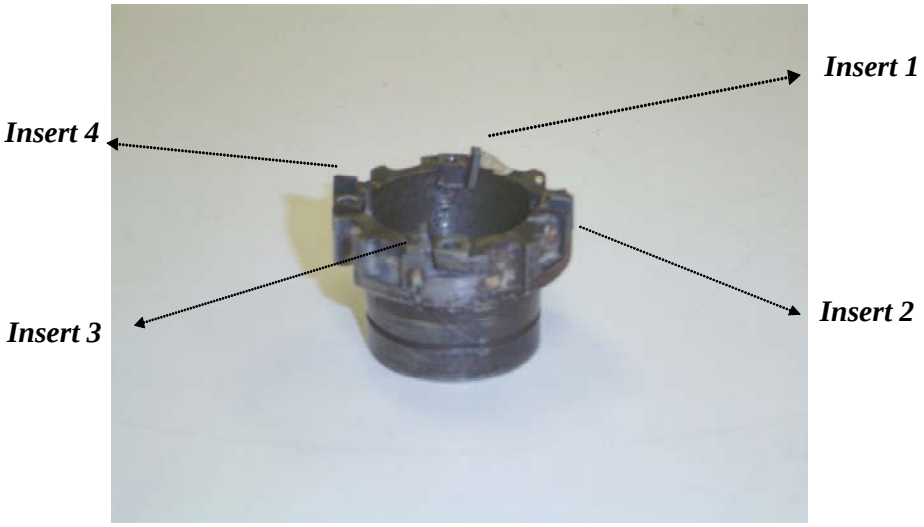

Figure 3.1: PCD compact core drill showing the four inserts

(Provided by Kris Zacny, Honeybee Robotics)

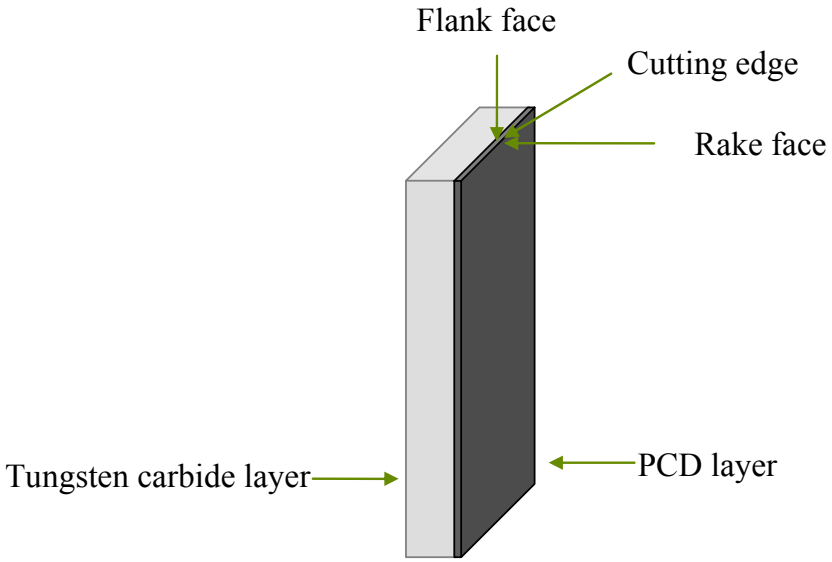

Figure 3.2: Isometric view of a single PCD compact insert

3.3 Experimental Set-up

The experimental setup used in conducting the core drilling experiments on basalt rock samples consists of a HAAS VF2 vertical machining center as shown in Figure 3.3, drill dynamometer, data acquisition system and a computer to record the data. The basalt rock sample is held to the machine bed by means of a purpose made fixture that is mounted on the drill dynamometer as shown in Figure 3.4. A hollow steel stem which is press fit into a collet is used to firmly hold the core drill as a single unit.

Figure 3.3: Experimental set-up for core drilling of basalt at University of Kentucky Machining Research Laboratory

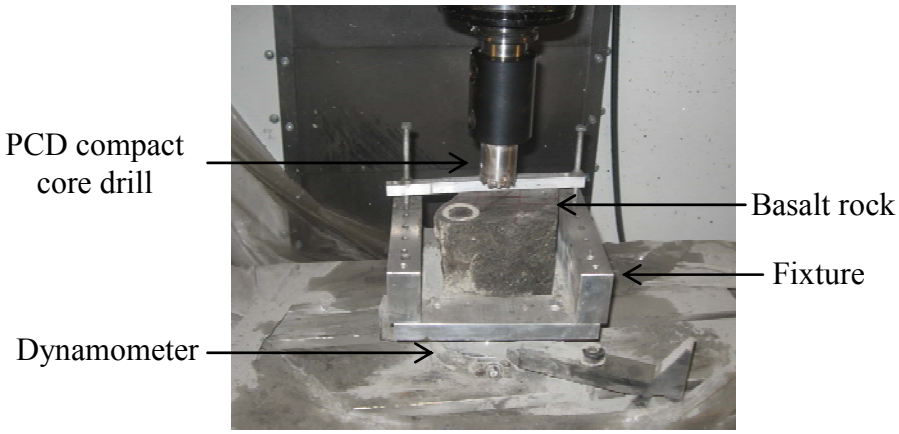

Figure 3.4: PCD compact core drill and basalt rock specimen fixed in the Haas vertical machining center

3.4 Preliminary Experiments

This section describes the observations made during the extensive preliminary experiments conducted to study the core drilling process in basalt rock.

3.4.1 Influence of Rock Powder

In order to determine drilling depth increment in basalt rock using the PCD compact core drill, several preliminary experiments were conducted to determine the drilling depth intervals in order to measure progressive tool-wear. Initially, experiments were carried out for a drilling depth increment of 10 mm; recording thrust force and torque during the tests. The torque data showed huge fluctuations when compared to the thrust force. The reasons for this will be discussed in the next sub-section. When the drilling depth is increased to 20 mm (another 10 mm in previous hole), the reaction torque suddenly increased in value at the end of the test as shown in Figure 3.5b. The rock powder generated during core drilling process is believed to have caused this increase. The use of cutting fluids to excavate the rock powder is less feasible on Mars than on Earth, due to low temperature and pressure of the Martian atmosphere. Due to this limitation, the maximum drilling depth increment between drill withdrawals of 15 mm is selected for the main stream of experiments.

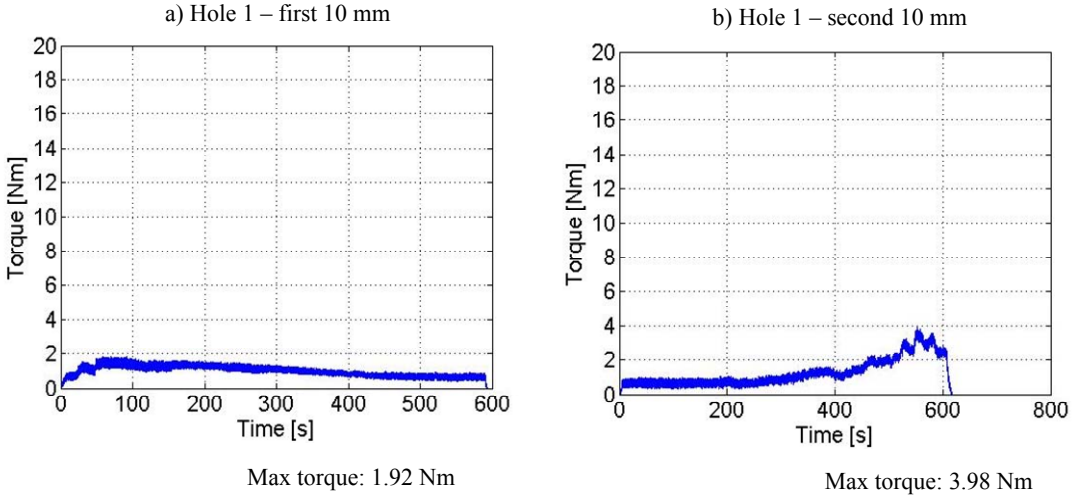

Figure 3.5: Torque data recorded during preliminary experiments

(Speed: 100 rpm, Feed: 0.01 mm/rev, Drilling depth: 20 mm, Rake angle: -10°)

Further, three sets of experiments were conducted with identical cutting conditions and rake angle at 15 mm drilling depth to verify the repeatability of the thrust force and torque data. The data show a variation of 2% for maximum thrust and torque recorded for a drilling depth of 15 mm.

3.4.2 Dynamic Behavior during Rock Drilling Process

As mentioned earlier, during the initial tests, the variation in the measured torque is large when compared to the thrust force signal as shown in Figure 3.6. A dynamic analysis of the core drilling apparatus is carried out to find the reasons for such behavior, while recording the torque data. The initial sampling frequency at which the data is gathered was 10 Hz. The variation in the torque signal recorded when a 15 mm hole is drilled, using PCD compact core drill, is observed to be 37%, whereas the variation in thrust force signal in the same experiment is just 4%.

The current data is gathered in the time domain, hence analyzing the data in the frequency domain using Fast Fourier Transform should show the frequency of the noise and vibrations present. These experiments were repeated at a sampling frequency of 200 Hz (higher sampling frequency is required to detect noise frequencies). Figure 3.7 shows the frequency analysis of the thrust and torque signal for 15 mm drilling depth in which amplitude of the frequencies in the torque and the thrust force are indicated. It can be clearly noted that the spindle vibrations (2.3 Hz corresponding to 100 rpm) are dominant in the torque signal.

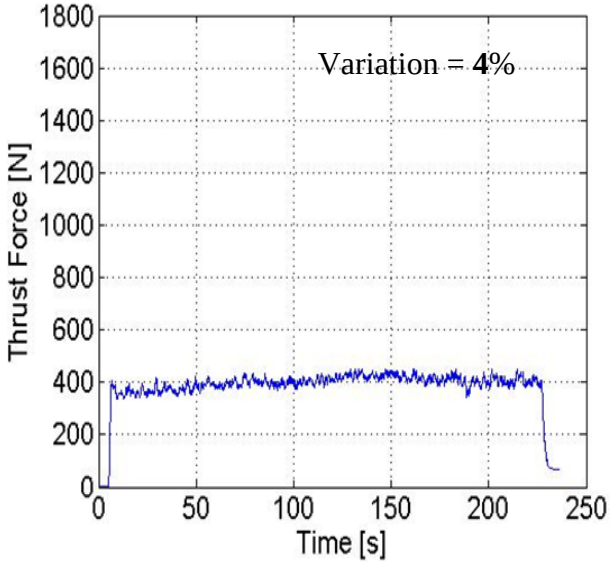

Max thrust force – 453 N

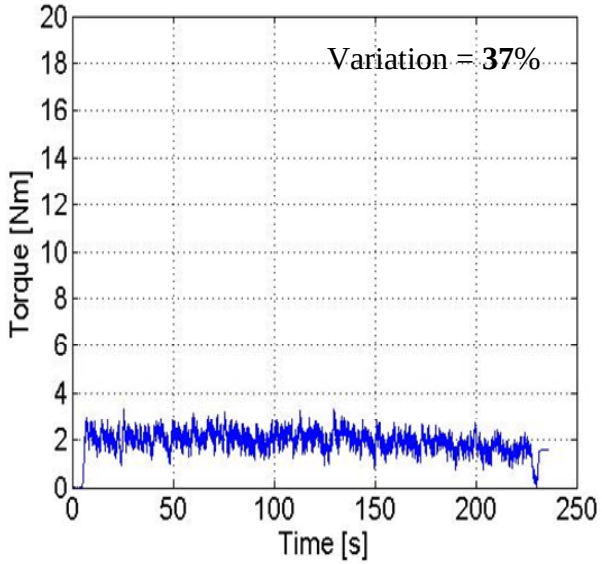

Max torque – 3.35 Nm

Figure 3.6: Sample thrust force and torque plots obtained during preliminary testing in sample basalt rock

(Speed: 140 rpm, Feed: 0.025 mm/rev, Drilling depth: 15 mm, Rake angle: -10°)

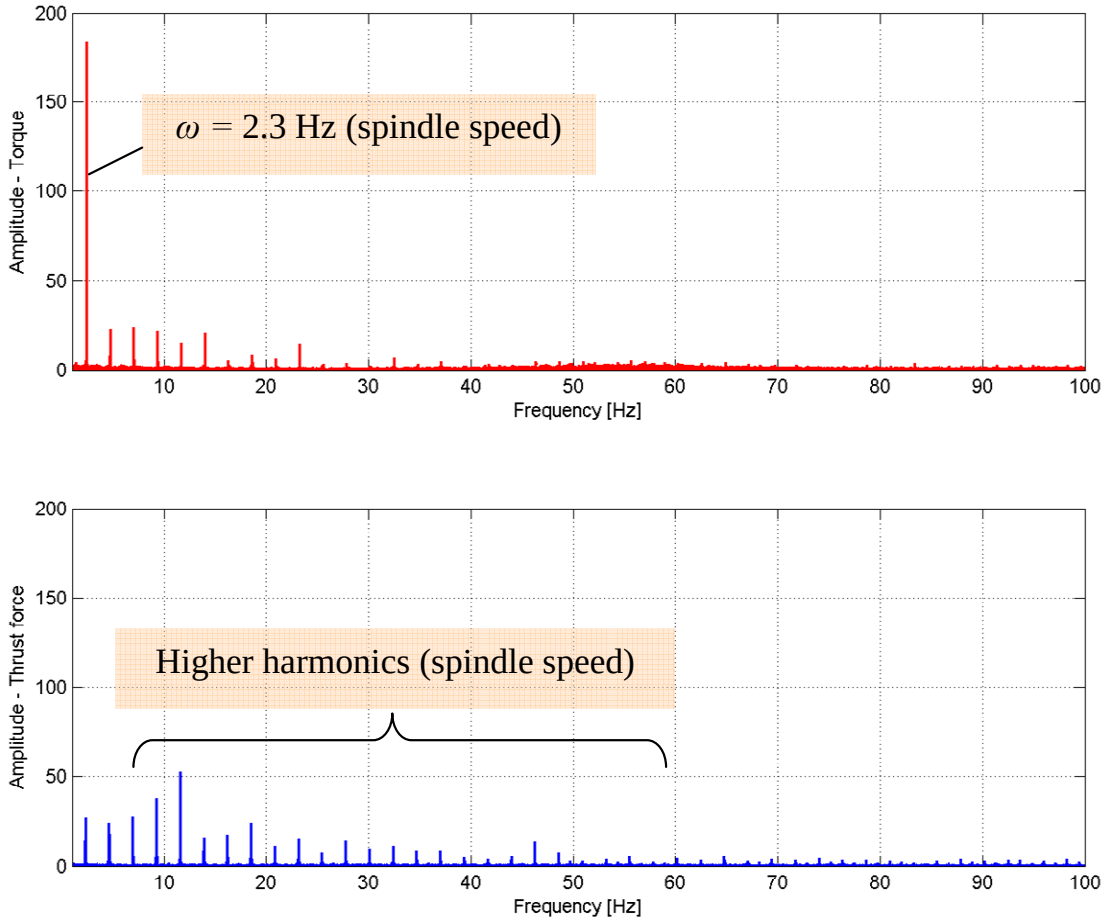

Figure 3.7: Analysis of thrust force and torque signals on frequency domain

The fluctuation in torque signal is reduced to 22% of mean value with the increase of sampling frequency; hence experiments were conducted at higher sampling frequencies of 2000 Hz. The results showed a significant drop in fluctuation in the torque signal to 13% of mean value, and peaks were observed at higher frequencies at around 650 Hz in the frequency domain as shown in Figure 3.8.

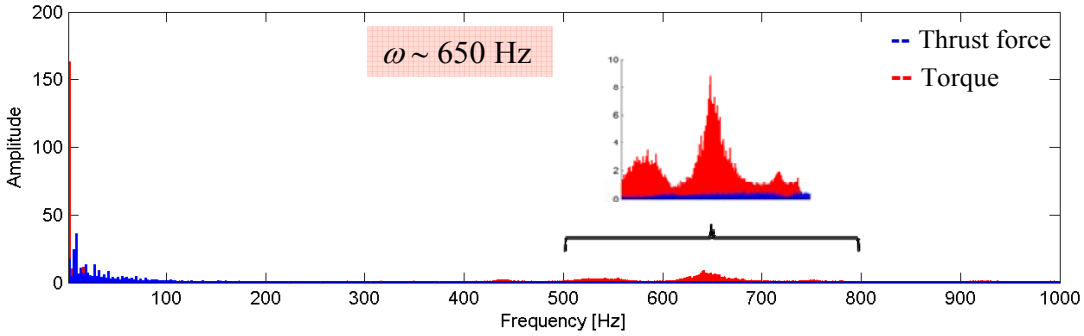

Figure 3.8: Frequency domain plots of thrust force and torque sampled at 2000 Hz

The modal analysis of the tool structure given in Appendix II showed that torsion resonance of the tool assembly is in the proximity of the above mentioned vibrations. Thus by reducing the size of the hollow steel stem length, the critical vibration frequencies can be avoided. Due to the memory limitations of the computer that is used to record the experimental data, the sampling frequency of 1000 Hz is selected for use during the rest of the core drilling experiments.

3.5 Experimental Procedure

In this section, the method employed to design the experiments for each parameter and its values and detailed explanation of measurement technique of the output parameters will be discussed. The sequential steps in which each experiment is conducted is also listed

here along with the brief description of the equipment used to obtain the data that is required for the optimization process.

3.5.1 Design of Experiments

The experiments for tool geometry and cutting conditions optimization are chosen using the Taguchi design of experiments principles (L16 orthogonal array).

Table 3.3 shows the parameters involved and various levels of cutting conditions selected to gather the experimental data for later use in the optimization procedure. The number of experiments required for 3 parameters at 4 levels using full factorial design of experiments will be 64 whereas the Taguchi method reduces the number of experiments to 16. Using this method, the variables are distributed in such a manner that all the variables are disturbed in same number throughout the 16 experiments, as shown in Table 3.4.

Table 3.3: Experimental matrix

Parameter	Level I	Level II	Level III	Level IV
Rake angle (deg)	-5	-10	-15	-20
Speed (rpm)	60	100	140	180
Feed (mm/rev)	0.01	0.025	0.04	0.05

The cutting conditions, speed and feed that are to be used are shown in Table 3.4. They are programmed in the vertical machining center that is used to conduct the drilling experiments. The initial rake angle at which the inserts are mounted is -10°; hence shims and wedges are prepared to establish the value of -5°, -15°, and -25° for the rake angles for the inserts when placed in the core drill.

Table 3.4: Taguchi design of experiments

Exp. No.	Rake angle (deg)	Speed (rpm)	Feed (mm/rev)
1	-5	60	0.01
2	-5	100	0.025
3	-5	140	0.04
4	-5	180	0.05
5	-10	60	0.025
6	-10	100	0.01
7	-10	140	0.05
8	-10	180	0.04
9	-15	60	0.04
10	-15	100	0.05
11	-15	140	0.01
12	-15	180	0.025
13	-25	60	0.05
14	-25	100	0.04
15	-25	140	0.025
16	-25	180	0.01

For each set of experimental conditions, thrust force, torque, tool-wear and edge radius are measured after 15 mm depth intervals during core drilling of basalt since it is also determined as suitable interval to measure tool-wear. Due to high compressive strength of the basalt rock, the maximum drilling depth is restricted to 75 mm for each experiment in order to avoid catastrophic failure of the core drill.

3.5.2 Thrust Force and Torque Measurement

A 4-component Kistler tool dynamometer is used to measure and record the thrust force and torque along with the HT-600 data acquisition system are shown in Figure 3.9.

Figure 3.9: A 4-component Kistler dynamometer and the HT-600 data acquisition system used to measure thrust force and torque

In addition to the dynamometer and data acquisition system, the thrust force/torque measuring system includes charge amplifiers which convert the input signals from the dynamometer into output voltages proportional to the forces sustained.

The dynamometer is initially calibrated using a dead weight of 75 N for force in the Z direction and a wrench that provides calibrated torque values ranging from 1 – 5 Nm at sampling frequency of 1000 Hz. Before beginning the drilling process, the charge amplifiers are reset to zero, which nullifies the mass of the fixture and rock, thus setting the reference value of the thrust force and torque measurements to zero. Typical thrust force and torque data recorded for the experiments is shown in Figure 3.10.

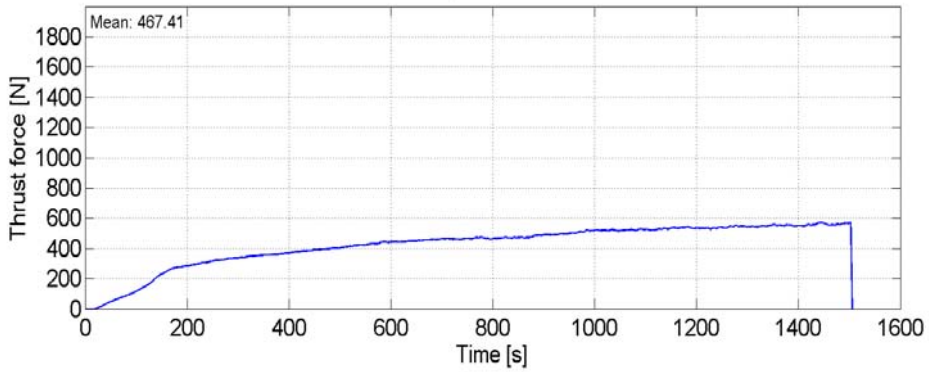

(a) Thrust force

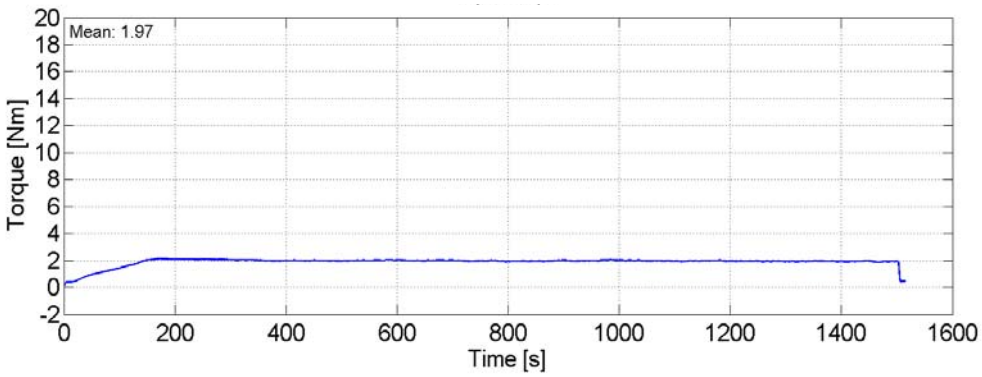

(b) Torque

Figure 3.10: Typical (a) thrust force and (b) torque measurements obtained while core drilling basalt Rock 1

(Speed: 60 rpm, Feed: 0.040 mm/rev, Drilling depth: 15 mm, Rake angle: –15°)

3.5.3 Tool-wear Measurement

To determine tool-wear the PCD compact inserts are manually removed from the core drill and observed using an Olympus BX41 system microscope along with a Olympus Qcolor3 digital camera at 200X magnification. Flank wear and rake face wear are

observed. Since flank wear is found to be the dominant tool-wear among these two, it is measured on all inserts after each 15 mm of drilling depth interval. Due to the random distribution of polycrystalline diamonds in the inserts and the abrasive nature of the rock cutting process (similar to grinding), the maximum flank wear is selected as the tool-wear criterion. Figure 3.11 illustrates the progressive flank wear data of one PCD compact insert ranging from 0 mm to 75 mm. The wear measurements are done using ImagePro, analysis software for images. Using this software tool, the worn surface of the insert can be represented between two lines and hence the distance between these lines is measured.

The length of each PCD insert is 3.5 mm and higher magnification reduces the area of focus, thus 3 measurements of maximum flank wear are taken and averaged for each insert. Finally, the core drill has four inserts mounted on it radially; hence the average of maximum flank wear of the inserts is calculated for each cutting condition.

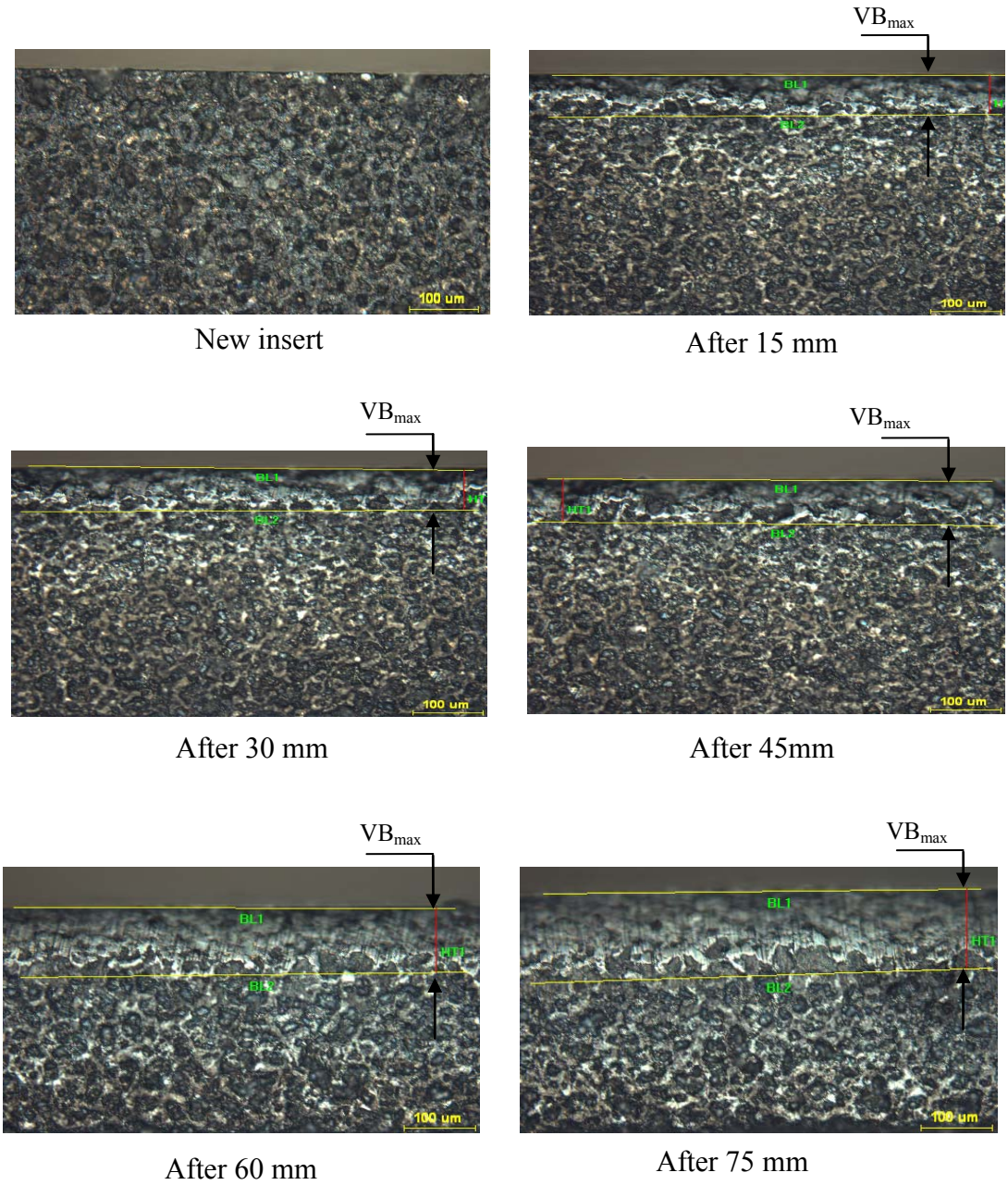

Figure 3.11: Progressive flank wear measurement of a PCD compact insert at 200X magnification

(Speed: 60 rpm, Feed: 0.040 mm/rev, Drilled depth: 75 mm, Rake angle: –15°)

The statistical variation in the maximum flank wear values among the four inserts for given cutting conditions is represented using an error bar plot in Figure 3.12.

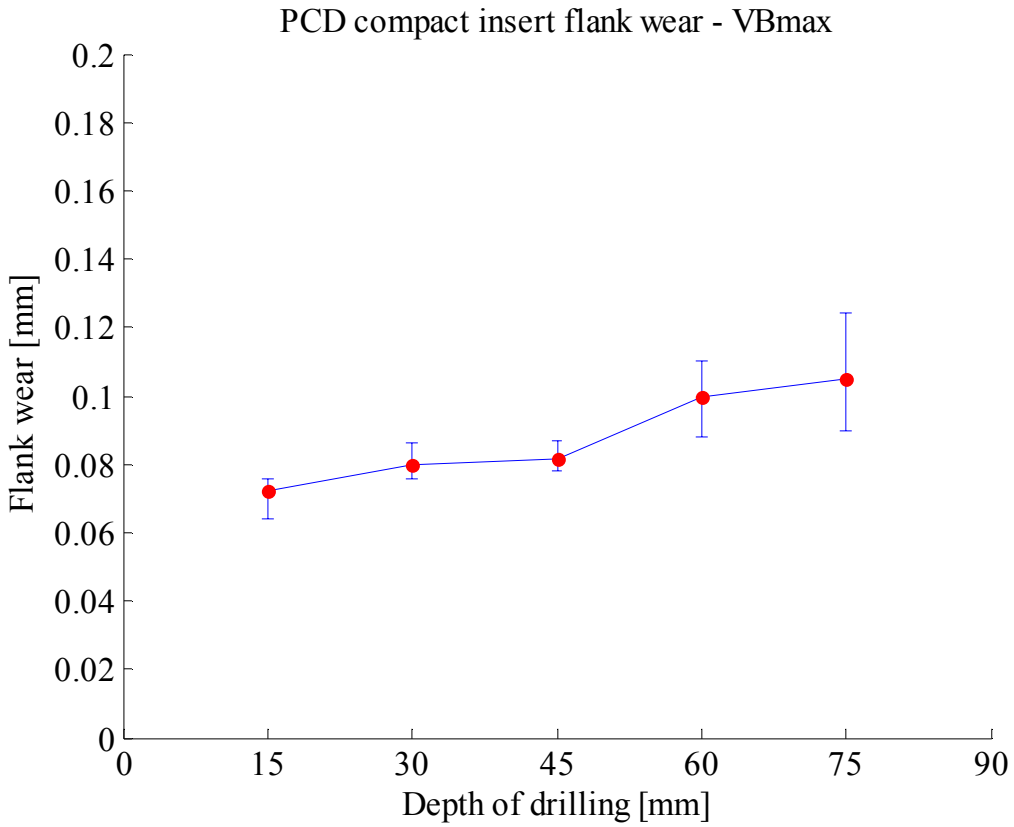

Figure 3.12: The variation in flank wear among the four inserts

(Speed: 60 rpm, Feed: 0.040 mm/rev, Drilled depth: 75 mm, Rake angle: –15°)

3.5.4 Edge Radius Measurement

The edge radius of the PCD compact insert represents the measure of roundness of the insert between the rake face and flank face at the cutting edge of the insert (see Figure 3.2). The edge radius of these inserts is measured using a Zygo interferometric microscope along with Metropro 8.0 analysis software. The new inserts are randomly selected for the experiments and the initial edge radius is measured. The technique and

the procedure followed to measure the edge radius of these tools at micro level are explained in the following paragraph.

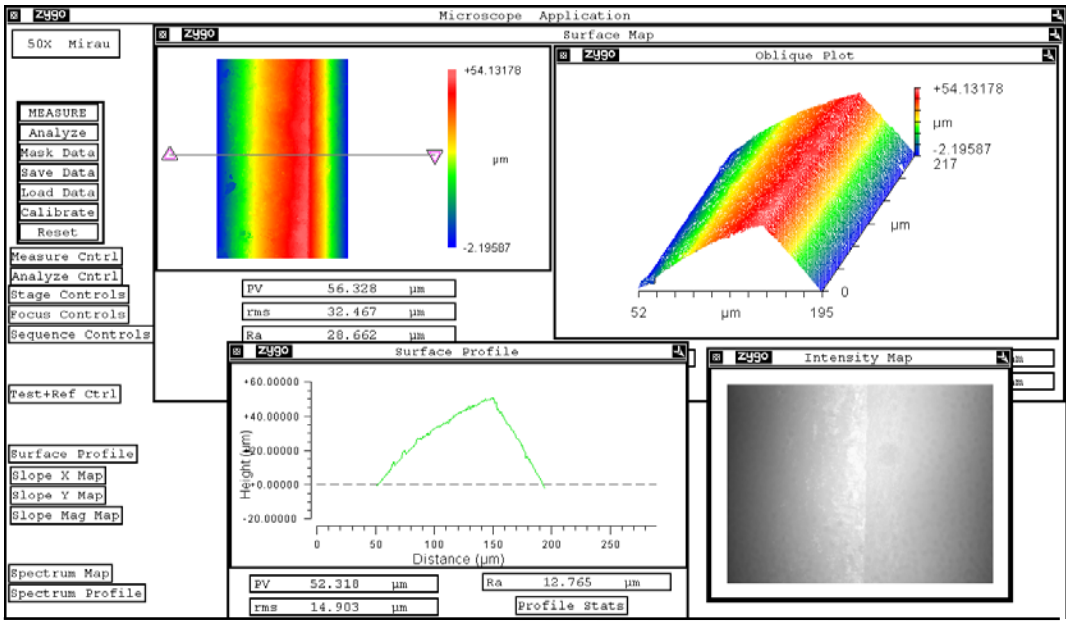

Figure 3.13: Screen shot of PCD compact insert cutting edge surface taken using Zygo interferometric microscope at 50X magnification

The insert is placed on a fixture that allows the light source from a Zygo microscope to impinge directly on the cutting edge. After capturing the surface of the cutting edge, a screen shot of the cutting edge profile is taken using Metropro analysis software. The three dimensional surface of the cutting edge involved in the drilling process whose edge radius is to be determined is captured at 50X magnification. Figure 3.13 shows an oblique plot of the cutting edge of a typical PCD compact insert, surface map and surface profile of the insert. The surface profile is a replot using Matlab software to determine the profile of the cutting edge radius. The typical edge radius profiles of the new and worn PCD compact inserts are shown in Figure 3.14.

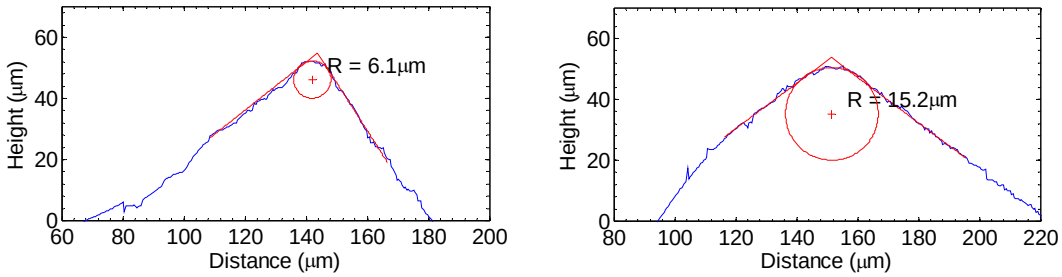

(a) New insert (b) Worn insert

Figure 3.14: Typical edge radius profiles of (a) New insert and (b) Worn insert after drilling 75 mm

(Speed: 60 rpm, Feed: 0.040 mm/rev, Drilled depth: 75 mm, Rake angle: –15°)

3.5.5 Step by Step Procedure to Conduct Core Drilling Experiment

A standard work procedure is followed as mentioned below to obtain consistent results throughout the experiments.

a) The basalt rock specimen is held firmly on the fixture and core drill is mounted in the CNC machine at the beginning of each experiment.

b) The experimental conditions derived from Taguchi design of experiments such as cutting speed and feed are set in the vertical CNC machine.

c) The data acquisition system is turned on, amplifiers are reset to zero and drilling is started.

d) The thrust force and torque are monitored, using the data acquisition system while core drilling the basalt rock for the 15 mm drilling depth, for each experimental condition.

e) The inserts are then removed and observed under microscope at 200x magnification for the tool-wear. The edge radius of each insert is then measured using a Zygo 3-D measuring system.

f) The inserts are then placed back on the PCD compact core drill to continue the drilling for another 15 mm.

g) The total drill depth achieved with each set of experimental conditions is 75 mm (i.e., 5 passes of 15 mm each).

CHAPTER 4

EXPERIMENTAL RESULTS AND OPTIMIZATION OF CORE DRILLING PROCESS

The experimental results composed of thrust force, torque, and flank wear are tabulated in order to develop an empirical model which will be further used for the optimization of the core drilling process in basalt rock. In the following sections, the discussion of the results obtained, development of a mathematical model based on tool-wear, determination of empirical constants using the experimental data and finally the optimization of cutting conditions in order to minimize the tool-wear of PCD compact core drill are discussed. These conditions are also believed to be the ones associated with minimizing the chances of drills breaking (Jawahir and Wang, 2007).

4.1 Analysis of Experimental Data

As mentioned in the previous chapter, the experiments are conducted on two basalt rock samples in such a way that all 16 experiments were done in a consistent manner. Hence the initial drilling depth of 30 mm in each experiment is conducted on basalt Rock 1, successive 30 mm on basalt Rock 2 and the fixed 15 mm in either of the rocks. The experimental data related to 60 mm drilling depth is used for analysis. After gathering the data from the experiments, the results are listed in tabular form as shown in Table 4.1 for further analysis. Mean, minimum and maximum thrust force are calculated from the thrust plots to relate the progressive tool-wear that is measured after 15 mm drilling depth. However the mean torque taken from the torque plots is used since torque is steady

throughout the experiments. The increase in the thrust force can be an indication of the tool-wear which is measured after the experiments. The typical plots showing the thrust force and torque required for given cutting conditions and rake angle are shown in Figure 4.1 and Table 4.1.

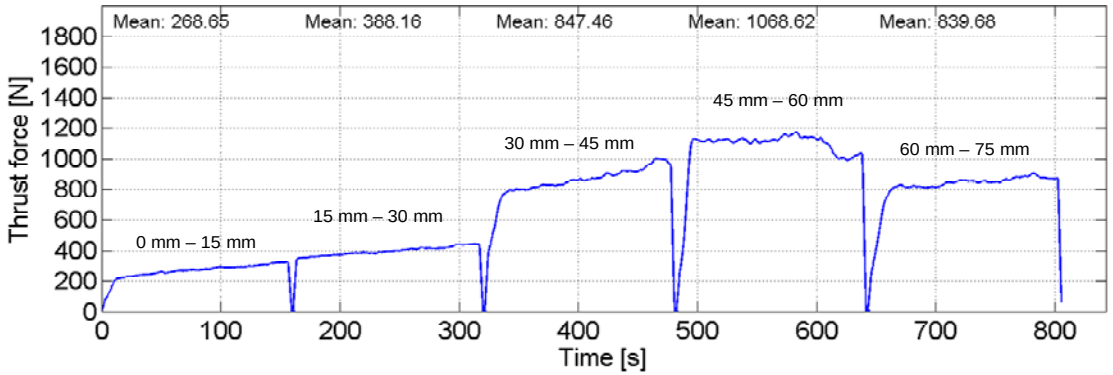

(a) Thrust force

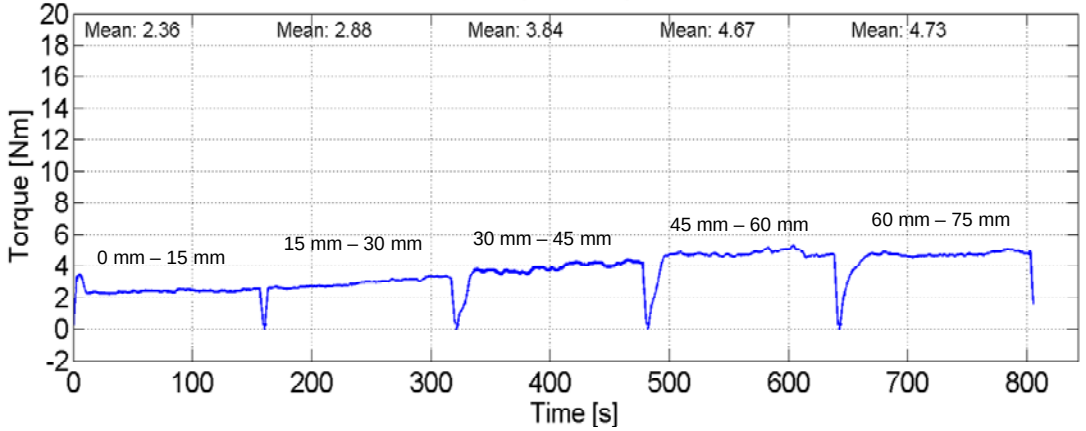

(b) Torque

Figure 3.10: Typical (a) thrust force and (b) torque measurements obtained while core drilling basalt

(Speed: 140 rpm, Feed: 0.040 mm/rev, Drilled depth: 75 mm, Rake angle: –5°)

Table 4.1: Experimental data obtained from Taguchi design of experiments

Exp	Rake angle (deg)	Speed (rpm)	Feed (mm/rev)	Drilling depth **[Mean Thrust force (N), Mean Torque (N-m), Max. Flank Wear (mm)]**														
				15 mm			30mm			45 mm			60mm			75mm		
1	-5	60	0.01	457	1.97	0.100	482	1.18	0.122	1070	3.00	0.173	1090	3.70	0.211	732	1.79	0.224
2	-5	100	0.025	401	3.12	0.088	397	2.58	0.101	823	4.23	0.141	1155	4.47	0.168	1100	4.83	0.182
3	-5	140	0.04	269	2.36	0.072	388	2.88	0.091	847	3.84	0.128	1069	4.67	0.145	840	4.73	0.155
4	-5	180	0.05	283	2.87	0.076	327	4.00	0.095	691	4.48	0.113	783	4.03	0.131	554	2.47	0.141
5	-10	60	0.025	424	3.17	0.058	420	2.94	0.078	895	4.54	0.120	1434	4.87	0.138	1041	3.11	0.147
6	-10	100	0.01	447	1.54	0.063	536	2.97	0.080	1232	4.14	0.138	1653	1.53	0.163	961	1.08	0.169
7	-10	140	0.05	308	3.21	0.063	288	2.67	0.074	709	5.24	0.094	880	6.75	0.098	569	4.30	0.108
8	-10	180	0.04	239	2.36	0.062	437	4.14	0.068	694	2.45	0.096	562	3.49	0.098	586	3.39	0.103
9	-15	60	0.04	344	3.45	0.072	476	3.89	0.080	749	5.74	0.081	1140	6.10	0.100	1198	5.15	0.105
10	-15	100	0.05	408	5.59	0.060	513	4.71	0.072	698	5.97	0.083	958	6.23	0.095	1066	6.23	0.099
11	-15	140	0.01	541	2.89	0.074	604	1.65	0.083	939	2.72	0.099	1325	1.54	0.112	1564	5.49	0.130
12	-15	180	0.025	251	2.65	0.067	354	1.39	0.074	408	3.80	0.081	818	3.8	0.091	979	5.26	0.103
13	-25	60	0.05	323	4.52	0.080	599	8.59	0.098	595	4.61	0.105	705	6.27	0.118	879	4.68	0.126
14	-25	100	0.04	340	4.22	0.083	575	7.26	0.096	613	4.92	0.107	817	5.06	0.127	897	3.25	0.141
15	-25	140	0.025	331	2.79	0.070	530	3.50	0.094	624	3.70	0.098	686	4.08	0.113	919	1.83	0.118
16	-25	180	0.01	350	1.25	0.068	439	2.21	0.077	811	2.89	0.096	1143	2.95	0.106	1312	1.18	0.113

The edge radius measurements of new PCD compact inserts are represented in the form of bar chart shown in Figure 4.2 in which 16 different colored bars correspond to the 16 experiments selected from design of experiments (see Table 4.1) criteria. Since four inserts are mounted in the core drill for each experiment, the insert number is selected as the x-axis. Thus the edge radius of inserts 1, 2, 3 and 4 is represented by the same color for each experiment. For instance, if dark red colored bar represents the edge radius of insert 1, 2, 3 and 4 which are selected to conduct drilling experiment 16 in Table 4.1; it is represented by all the last columns in Figure 4.2. Due to small variation in the cutting edge radii of new inserts, it can be assumed that all the new PCD compact inserts have equal edge radius.

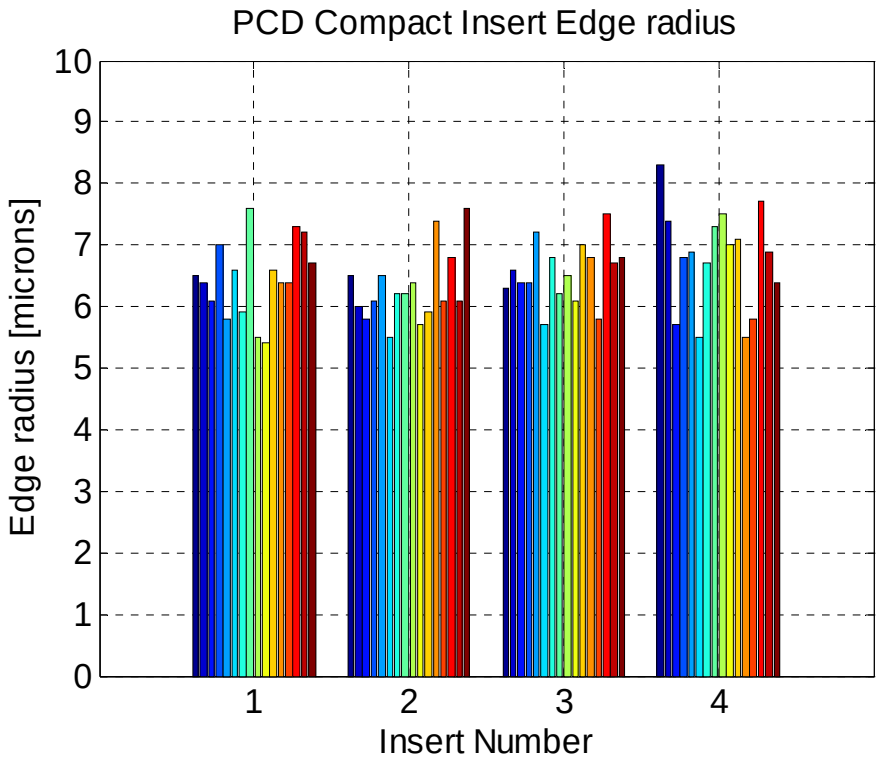

Figure 4.2: Statistical variation in edge radius measurements of new PCD compact inserts

4.1.1 Influence of Rock Properties

In this section, the difference in behavior of the thrust forces from one rock sample to another rock sample and the influence of rock powder created during drilling will be analyzed from the thrust force plots. Consider the typical plot of thrust force shown in Figure 4.1 for a drilling depth of 45 mm. The first 30 mm was in basalt Rock 1 and then an additional 15 mm of drilling in basalt Rock 2. The details of the measured thrust force plots are shown in Figure 4.3.

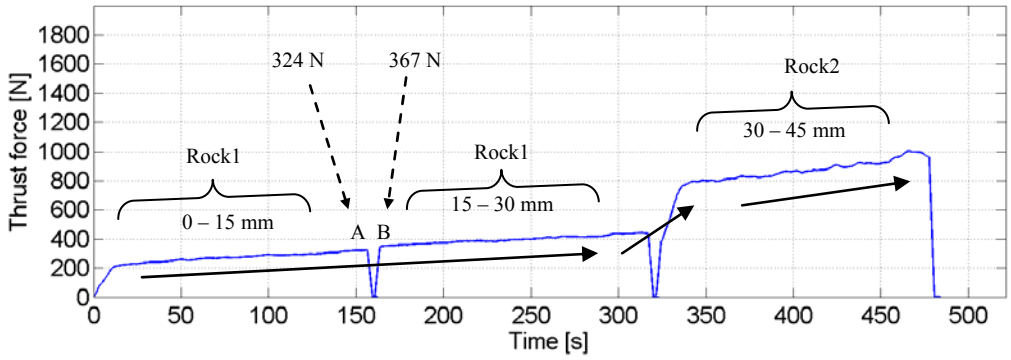

Figure 4.3: Detailed thrust force plots for a drilling depth of 45 mm during core drilling in basalt for high feed condition

(Speed: 140 rpm, Feed: 0.04 mm/rev, Drilled depth: 45 mm, Rake angle: –5°)

It can be observed that the thrust force required to core drill basalt Rock 2 at the specific feed increases rapidly after 30 mm of drilling in Rock 1, since the compressive strength of Rock 2 is greater than that of Rock 1. The rate of increase in thrust force is also large in Rock 2 when compared to Rock 1 for the same drilling depth of 15 mm which also implies that the rate of tool-wear in Rock 2 is higher. Hence, monitoring the thrust force

will assist in the determination of some data of tool-life without actually looking directly at the drill bit.

Rock powder created during the core drilling process (instead of classical chips) also causes a slight increase in the required thrust forces when it accumulates around the bit. Figure 4.4 shows a selected portion of the experimental thrust force plots during 45 mm of drilling that are similar to Figure 4.3, but for lower feed conditions. In this case, the minimum thrust force required to core drill from 15 mm to 30 mm is less than the maximum thrust force recorded at the end of 15 mm drilling depth.

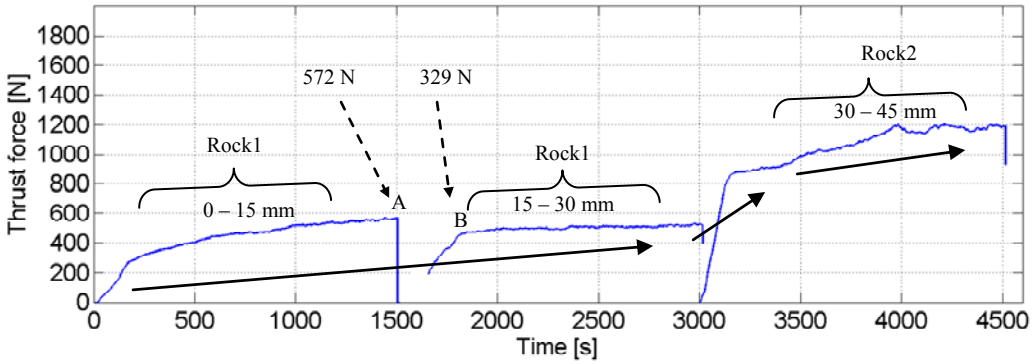

Figure 4.4: Detailed thrust force plots for a drilling depth of 45 mm showing the influence of rock powder for low feed condition

(Speed: 60 rpm, Feed: 0.01 mm/rev, Drilled depth: 45 mm, Rake angle: –5°)

This shows the influence of rock powder created (plus wear) in the first 15 mm of drilled depth, the initial required thrust force for successive 15 mm decreases by 243 N between points A and B for such conditions. For the high feed conditions shown in Figure 4.3, no

similar increase is noticed. Therefore, the rock powder influence is more evident at low-feed conditions than in high feed conditions.

Using the experimental data mentioned above in Table 4.1, the drilling power can be calculated and empirical models for thrust force and power can be established as described below.

4.1.2 Calculation of Drilling Power

The power required to perform core drilling on planet Mars will be supplied by batteries or solar energy. Thus power is a major constraint in the current application and so it is imperative to calculate the power consumed in the drilling experiments conducted in this investigation. Zacny and Cooper (2007) used similar core drill on basalt rock samples, hence derived an empirical equation to calculate the drilling power (W) in their most recent investigation. The equation for drilling power is shown below (Zacny and Cooper, 2007),

$$Power_{drilling} = UCS \times Area \times Feed \times \left(\frac{2\pi \times RPM}{60} \right) + Torque \times \left(\frac{2\pi \times RPM}{60} \right) \qquad (4.1)$$

where, UCS = Uni-axial compressive strength (MPa), Area = $\frac{\pi}{4}\left(OD^2 - ID^2\right)$, OD = outer diameter in mm, ID = inner diameter in mm, Feed = depth of cut per revolution, RPM = rotational speed in revolutions per minute.

From the Equation 4.1, drilling power can be estimated if speed, feed and the compressive strength of the rock that is being drilled are known. The compressive strength of the rock can be approximately determined by using the recorded thrust force and flank wear measurements. Zacny and Cooper (2007) have quoted that the stress required to break the rock is approximately equal to the compressive strength of the rock. Now, the stress applied on the rock can be determined by simple equation (Zacny and Cooper, 2007),

$$UCS = \left(\frac{Thrust\ force}{4 \times Flank\ wear \times length\ of\ the\ insert} \right) \tag{4.2}$$

The measured minimum thrust force and the calculated power for drilling depth of initial 15 mm are tabulated as shown in Table 4.2 for various cutting conditions.

Table 4.2: Measured minimum thrust force and calculated drilling power for initial 15 mm depth of drilling in Rock 1

Exp. No.	Speed (RPM)	Feed (mm/rev)	Minimum thrust force (N)	Drilling power (W)
1	60	0.01	265	23.44
2	100	0.025	287	97.64
3	140	0.04	231	218.70
4	180	0.05	243	351.49
5	60	0.025	200	58.59
6	100	0.01	239	39.08
7	140	0.05	171	273.36
8	180	0.04	225	281.21
9	60	0.04	208	93.74
10	100	0.05	174	195.28
11	140	0.01	198	54.69
12	180	0.025	288	175.74
13	60	0.05	189	117.19
14	100	0.04	218	156.26
15	140	0.025	252	136.71
16	180	0.01	218	70.33

4.1.3 Empirical Model for Drilling Power and Thrust Force

Thrust force is one of the major constraints in Martian applications because the magnitude that is available depends on the mass of the Rover or Lander used. For instance, if the mass of Rover is 500 kg, the maximum thrust force that can be applied in experiments conducted on Earth will be 1500 N (Zacny and Cooper, 2006). Due to such limitation, it is essential to know about the minimum thrust force needed during core drilling experiments there will be. In addition to thrust force, the required torque must be measured. Torque is defined as the product of tangential force and effective radius of the bit. The resultant of this tangential force and thrust force at the rock-bit interface determines whether the drill bit can achieve the required rate of penetration (Rao and

Misra, 1995). The extent of drill bit wear can be estimated by observing the thrust force and torque readings.

Since thrust force and power are major constraints while drilling on Mars, empirical models are developed to correlate the influence of the cutting conditions and geometry. For a given torque, drilling power is directly proportional to rate of penetration (speed x feed). Thus the data in Table 4.2 has a linear fit for drilling power against feed (mm/rev) is a good representation of the data shown in Figure 4.5. The linear equation for drilling power will be used in the optimization process below.

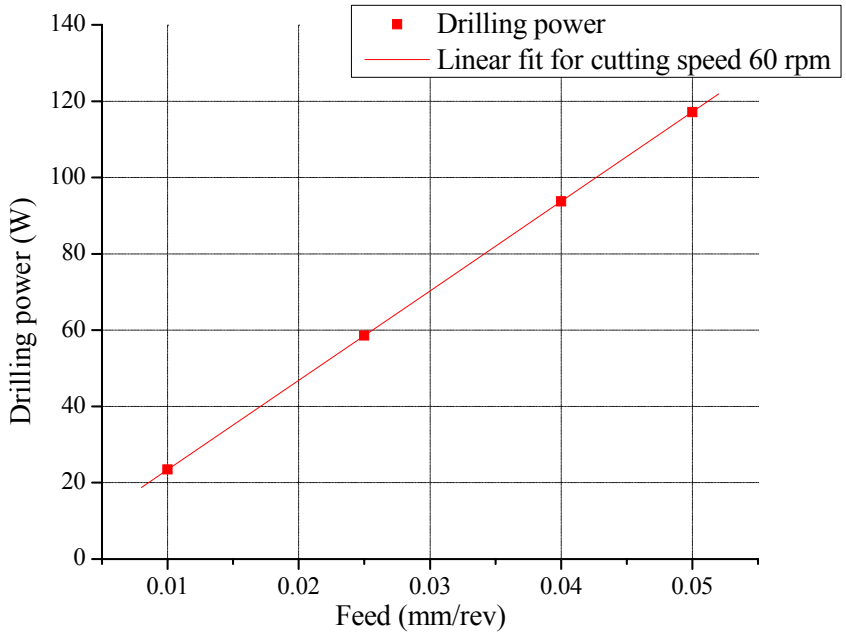

Figure 4.5: Linear fit of drilling power against feed for the cutting speed - 60 rpm in core drilling process of Rock 1

The data points in Table 4.2 representing the minimum thrust force for different feed values at constant cutting speed are fit using a quadratic equation. Similarly, minimum thrust force is plotted for various cutting speeds at constant feed. Figure 4.6 shows a sample quadratic fit of minimum thrust force against all the feed conditions at speed of 140 rpm carried on Rock 1. The trend can be shown to be similar for the cutting speeds 60 rpm, 100 rpm and 180 rpm for Rock 1. Similarly the curve fitting for minimum thrust force data at different cutting speeds at constant feed of 0.01 mm/rev for Rock 1 can be represented using quadratic equation. Therefore, the final empirical Equation 4.1, is determined by the multiple regression analysis of minimum thrust force data for given cutting conditions and used in the optimization model.

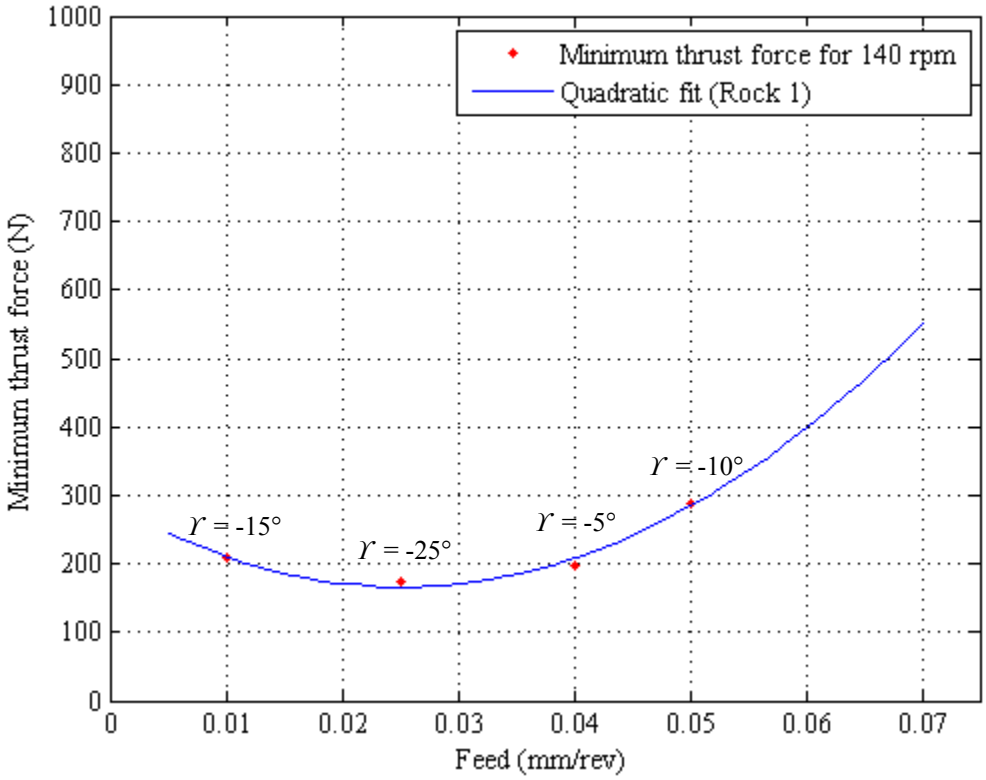

Figure 4.6: Quadratic-fit for minimum thrust force data for Rock 1 for cutting speed, 140 rpm

4.2 Tool-wear Model

After analyzing the forces and torque, the next logical step involved in the evaluation of the performance of any drilling operation is modeling the tool-wear. Since the rate of tool-wear determines the condition of the drill bit, which is crucial when drilling on Mars. It is reasonable to know the rate of tool-wear as the drill bit progresses into the Martian simulant, basalt. Work has been done in developing abrasive tool-wear models for polycrystalline diamonds considering the flank wear (also called wear flat) by measuring the cutting forces and temperature. Glowka (1985) has studied the influence of PCD compact tool temperature on rate of increase in flank wear.

In the current investigation, the temperature of the tool will increase as the wear on the core drill increases due to the absence of a coolant. Appl et al. (1996) proposed a theoretical model of diamond wear rate correlating the cutter forces and temperature with the flank wear of the tool. The flank wear rate generally increases with PCD compact cutter temperatures and is assumed to follow a linear relationship (Wilson and Vorono, 2003). Theoretical and empirical models are available in the literature for diamond tools used in rock machining processes such as grinding, sawing and cutting. However, the process of cutting rock in the above mentioned methods is confined to a crushing operation (Ilio and Togna , 2003).

Having a prediction scheme of drilling performance measures is a prerequisite for the optimization process. Empirical or analytical models studying the progressive wear phenomenon and its effects on the performance of core drilling hasn't been studied for

highly igneous rock basalt. Hence an attempt has been made to develop an empirical tool-wear model for PCD compact tools based on the experimental data gathered in this investigation. Since progressive tool-wear in polycrystalline diamond tools is produced by temperature dependent mechanism and influenced by the drilling time and rock material removal rate. The extended Taylor equation is usually considered a good approximation to correlate the tool life expressed in terms of cutting speed, feed, and depth of cut. Thus tool-wear can be approximately correlated using the following equation,

$$W = K \cdot V^{a} \cdot f^{b} \cdot d^{\theta} \tag{4.3}$$

where *W, V, f,* and *d* are the tool-wear, cutting speed, feed and drilling depth respectively and a, b, θ and *K* are empirical constants (Alauddin and El Baradie, 1997). The cutting speed *V* for the core drill can be calculated using the following equation (Lee et al., 1998),

$$V = \frac{\pi \cdot \mathrm{D} \cdot \mathrm{N}}{1000} \quad \text{m/min} \tag{4.4}$$

where N = cutting speed in rpm and D = effective diameter of the PCD compact core drill is 31.5 mm.

By including the geometry parameter rake angle in the Equation 4.3, the tool-wear can be further correlated as follows:

$$W = K \cdot V^{a} \cdot f^{b} \cdot \gamma^{c} \cdot d^{\theta} \tag{4.5}$$

where *W, V, f,* γ and *d* are the tool-wear, cutting speed, feed, negative rake angle and drilling depth respectively and *a, b, c,* θ and K are empirical constants.

From Equation 4.5, if the upper limit for wear is chosen, the maximum drilling depth (after evacuating the rock powder effectively) can be determined by,

$$d_{\max} = \left(\frac{W_{\max}}{K \cdot V^{a} \cdot f^{b} \cdot \gamma^{c}} \right)^{1/\theta} \tag{4.6}$$

where, W_{max} = tool-wear criterion (mm), V = cutting speed (m/min), f = feed rate (mm/rev), γ = negative rake angle (degrees), d = drilling depth (mm), *K, a, b, c,* θ = empirical constants.

To determine the tool-wear criterion (W_{max}) for PCD tools when core drilling hard and abrasive materials, a fixed value of the tool-wear is needed beyond which the tool is considered unusable or requires more cutting force than is available as in current situation. Davim and Antonio (2001) measured maximum flank wear in the drilling tests made using PCD tools in machining composites. These authors have identified the wear of the tools through flank wear and thereby optimized the drilling performance using genetic algorithms.

Table 4.3: Tool-wear data measured during the experiments carried upon by mounting PCD compact inserts at -5° rake angle

S. no	Speed (rpm)	Feed (mm/rev)	Drilling depth [Flank wear (mm)]				
			15 mm	30 mm	45 mm	60 mm	75 mm
Exp1	60	0.01	0.100	0.088	0.072	0.076	0.122
Exp2	100	0.025	0.101	0.091	0.095	0.173	0.141
Exp3	140	0.04	0.128	0.113	0.211	0.168	0.145
Exp4	180	0.05	0.131	0.224	0.182	0.155	0.141

In the current investigation flank wear is observed to be the dominant form of tool-wear when core drilling basalt rock using PCD compact drill bit under dry conditions. It is selected as a tool-wear criterion in the optimization model. The flank wear data is plotted against drilling depth as shown in Figure 4.7 for the experiments carried out using a -5° rake angle. The cutting conditions selected for these experiments are listed in Table 4.3. The plots clearly show the linear trend between the tool-wear with the depth of drilling. The error bars in Figure 4.7 for several combinations of cutting conditions indicate the variation in flank wear among the four inserts with respect to the average measurement of flank wear. Hence, multiple regression analysis has been adapted for the empirical model developed to correlate the tool-wear on PCD compact core drills.

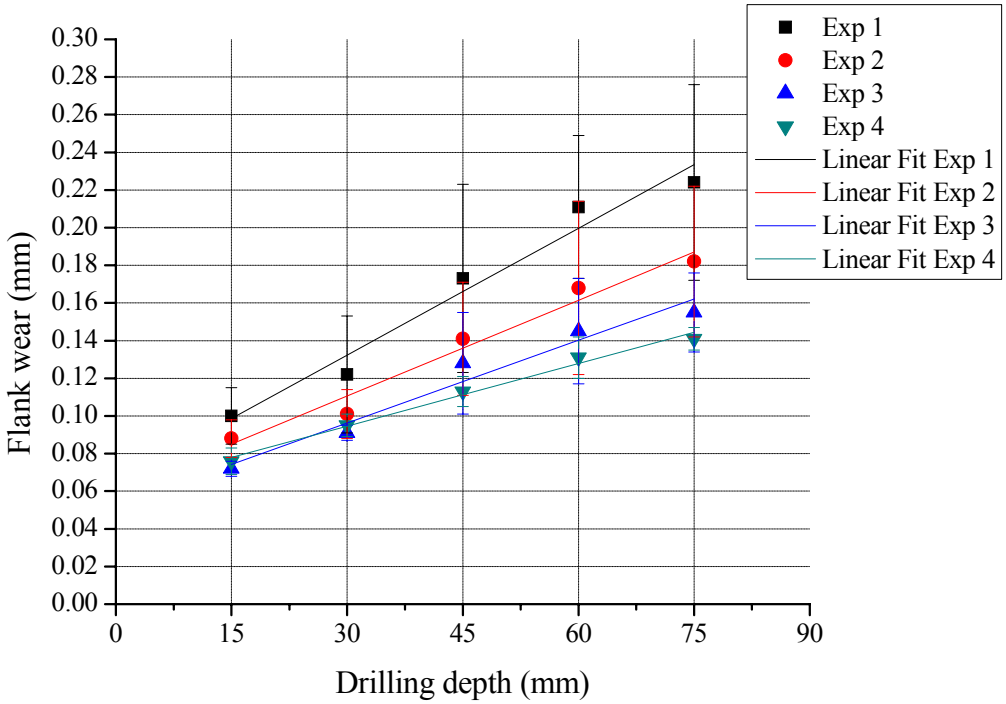

Figure 4.7: Plot showing linear relationship between flank wear against drilling depth for a rake angle -5 ° when drilling basalt with PCD compact core bit

The empirical constants were calculated by multiple regression analysis using "Microcal Origin 7.5" statistical analysis software from Originlab. The values of the empirical constants so determined after running several iterations and eliminating the outliers among the data points which are listed in Table 4.1 are given below:

a = -0.17294,

b = -0.10899,

c = -0.16488,

θ = 0.39464,

K = 0.03639.

4.3 Methodology of Optimization Process

The operating parameters initially selected to perform core drilling experiments may turn out to not be the optimum conditions to obtain minimum tool-wear for the given drilling depth. Tool wear/tool-life estimates are among the most required data for optimization of any machining process (Wanigarathne et al., 2005). The lack of experimental data and analytical relationships for the performance measures has identified the use of the optimization techniques in core drilling. Significant experimental data consisting of tool-wear for various cutting conditions is needed to develop the empirical models for the process of optimization. Models have been developed to predict the thrust force and power requirements to obtain core samples of various rock materials, but the study the progressive tool-wear for varying cutting conditions relevant to Martian basalt drilling applications has not been previously addressed.

The necessity for selection of optimal cutting conditions and geometry for the cutting tools to increase the tool-life, in any machining operation, has been focused by the researchers. Wang and Jawahir (2002) developed a comprehensive optimization criterion for turning operations using genetic algorithms to select the best cutting conditions and tool geometry by studying the effect of progressive tool-wear. In subsequent work, Wang and Jawahir (2005) designed a web-based optimization program which allows users to determine the optimum cutting conditions in milling operation based upon the empirical equations.

Recently, Jawahir and Wang (2007) developed methodology involving hybrid predictive optimization techniques for machining operations in general. The authors have discussed the methodology involved in optimization of various machining operations such as multi-pass turning, milling etc. Drilling performance can be predicted in terms of tool life, thrust force and torque by the process parameters such as drill diameter, cutting speed and feed (Lee et al., 1996; Davim and Antonio, 2001). The Taguchi method has been applied by Davim and Antonio (2001) to optimize cutting parameters in drilling of glass fiber reinforced composite (GFRC) material using the analysis of variance (ANOVA) to study the effect of varying drilling parameters.

To determine the optimal process parameters, an objective function has to be defined. The role of the objective function in optimization of core drilling operations is important due to the complex interactions among the selected variables that occur in the process. Since wear of the tool is an important criterion for the determination of drilling performance of the core drilling process, maximum tool-life and quantity of rock material removal should be considered when optimizing drilling performance.

The major constraints of drilling power and thrust force in the present investigation are selected based upon the ongoing strategic development for missions to Mars. The rock abrasion tool used for 2003 Mars Exploration Rovers is provided with a power of 150 W for drilling purposes (Zacny and Cooper, 2006). Even though the thrust force available for future missions might be approximately 1500 N (Zacny and Cooper, 2006), the minimum thrust force of 200 N, to start the actual drilling, is selected considering the

fraction of the mass of the Lander/Rover available to apply the thrust force. Basalt rock has been successfully core drilled with a minimum thrust force of 500 N by Zacny and Cooper (2007), over a depth of 15 cm resulting in a flank wear of approximately 0.2 mm. However, in their investigation, the thrust force is increased to 950 N to obtain the drilling depth of 15 cm. The maximum flank wear observed during the current experiments is 0.22 mm, thus W_{max} in the objective function has be set to a safe value which is chosen to be therefore 0.2 mm. This allows one to determine the corresponding maximum drilling depth.

The constraints selected for cutting speed, feed and rake angle are provided by the core drill supplier (Zacny, Honeybee robotics) by considering the safe cutting conditions and range of geometry so as to avoid the catastrophic failure of the PCD compact inserts. Rock material removal rate can be expressed in terms of the total drilling depth, thus the objective function can be stated as follows:

Objective function: Maximize the drilling depth *d (V, f, γ)* with respect to *V, f, γ*

where $d(V, f, \gamma) = \left(\frac{W_{\max}}{K \cdot V^{a} \cdot f^{b} \cdot \gamma^{c}} \right)^{1/\theta}$

Subject to the following constraints:

$P \leq 150$ (Watts) drilling power

$F_N \leq 900$ (N) thrust force

$6 \leq V \leq 18$ (m/min) cutting speed

$0.01 \leq f \leq 0.05$ (mm/rev) feed

$-5 \leq \gamma \leq -25$ (deg) rake angle

4.4 Results and Discussion

After developing the objective function and defining the constraints, an exhaustive enumeration methodology has been used to develop the optimization program using Matlab version 7.5 (R14). The sample Matlab code used for the optimization program is mentioned in Appendix III. The regression coefficients which are calculated using Equation (4.5) are substituted into Equation (4.6) to determine the tool-life response curve in terms of drilling depth for varying cutting speed, feed and rake angle. The 3-D plot for this response is shown by means of a slice plot in Figure 4.8.

The X axis represents the cutting speed (m/min), the Y axis represents feed (mm/rev) and the Z axis represents rake angle (deg) in Figure 4.8. The different bands in the slice plot show the drilling depth as predicted by the optimization model. The optimum point is

indicated by the yellow region at the intersection of three planes as determined by imposing the constraints in the tool-wear model. The three planes represent the speed, feed and rake angle at which the optimum total drilling depth (in 15 mm increments) is obtained by the tool-wear model. The vertical bar on the right hand side of the plot represents the scale of drilling depth values shown in the slice plot.

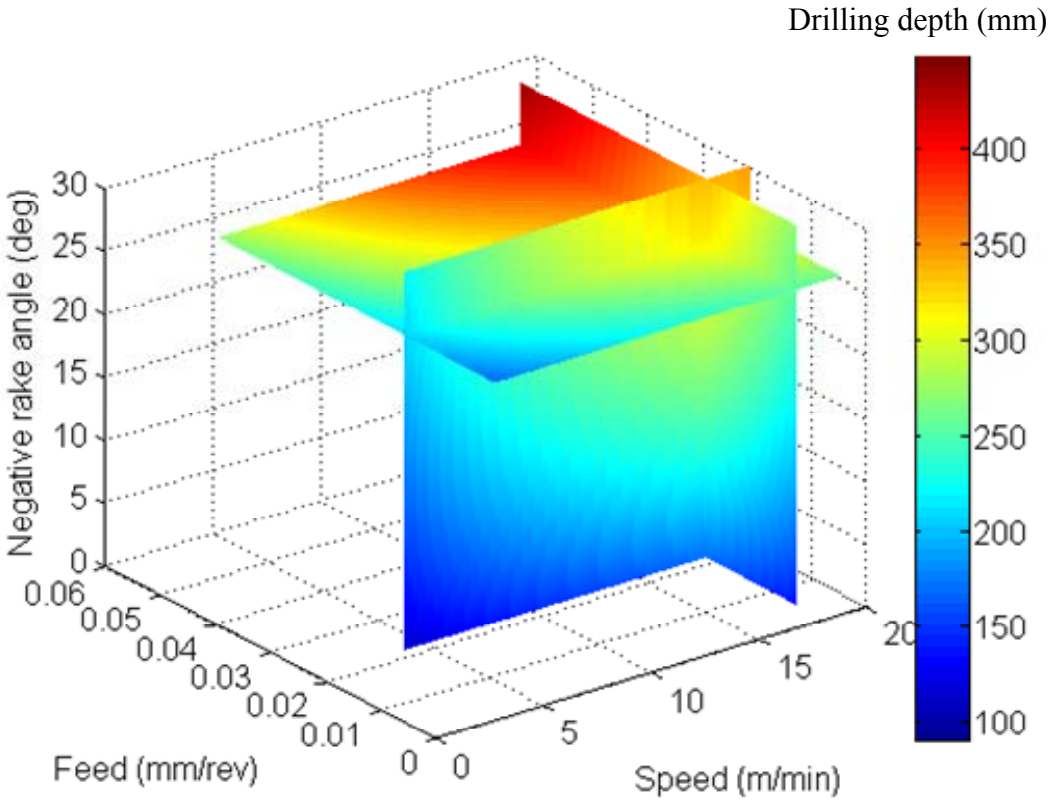

Figure 4.8: 3-D Representation of speed, feed and rake angle optimization

The 2-D representation of the three planes in Figure 4.8 can be useful in interpreting the optimization results. Thus 2-D contour plots are generated using Matlab to study the relationship between speed, feed and rake angle at optimum conditions. The 2-D contour plot representing the tool-wear response curve with respect to speed and feed showing the constraints drilling power and minimum thrust force is denoted by Figure 4.9. In other

words, this plot is a two dimensional view of one of the three planes in Figure 4.8 which is parallel to XY plane (X denotes speed, Y denotes feed).

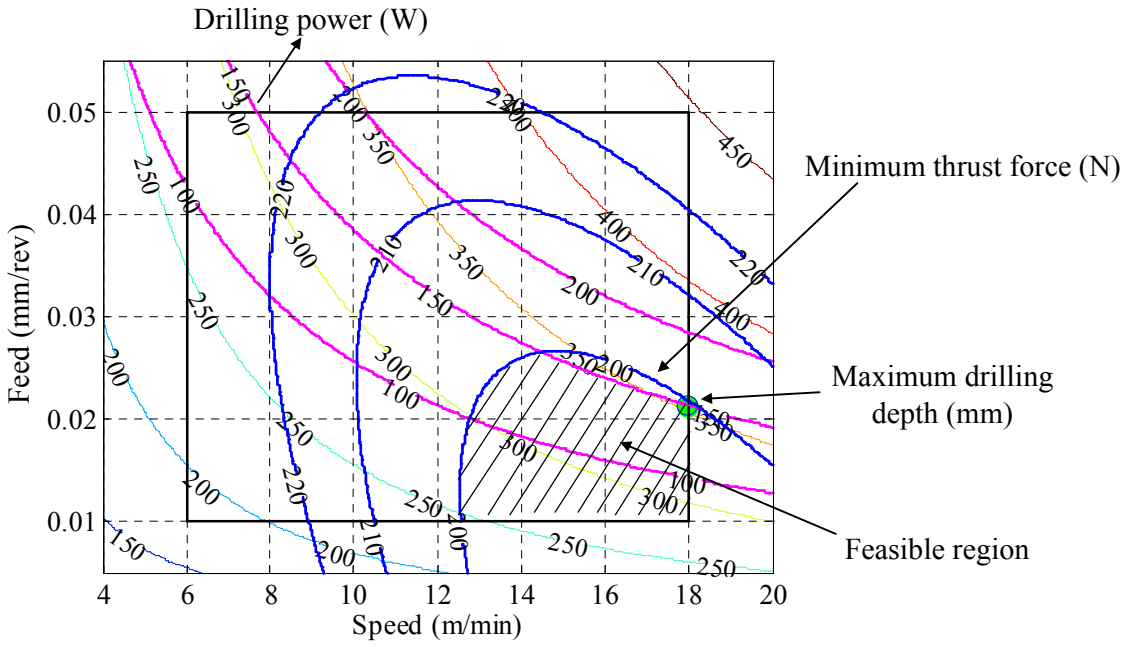

Figure 4.9: 2-D contour plot for speed and feed (XY plane in slice plot)

In Figure 4.9, the shaded region shows the feasible region for indicating the possible speed and feed conditions for drilling power of 150 W and minimum thrust force is 200 N. These constraints are shown in Figure 4.9, blue curve represents the minimum thrust force constraint of 200 N calculated from quadratic equation which is shown in shown in Appendix IV. The magenta curve shows the drilling power constraint for 150 W, which is also calculated for each speed-feed condition by using the empirical relation developed between drilling power and cutting conditions. The sample calculation is shown in Appendix IV. The green dot in Figure 4.9 shows the optimum drilling conditions at which maximum drilling depth can be achieved. Thus the maximum drilling depth

predicted by the optimization model for the core drilling operation is 350 mm (at intervals of 15 mm) and is achieved at high speed but low feed conditions.

The 2-D contour plot showing the tool-wear response curve plotted between rake angle and feed at optimum speed is shown in Figure 4.10. The rectangular region indicates the range of the selected parameters in the current investigation and the red dot indicates the optimum point (rake angle, feed) at which the maximum drilling depth is achieved.

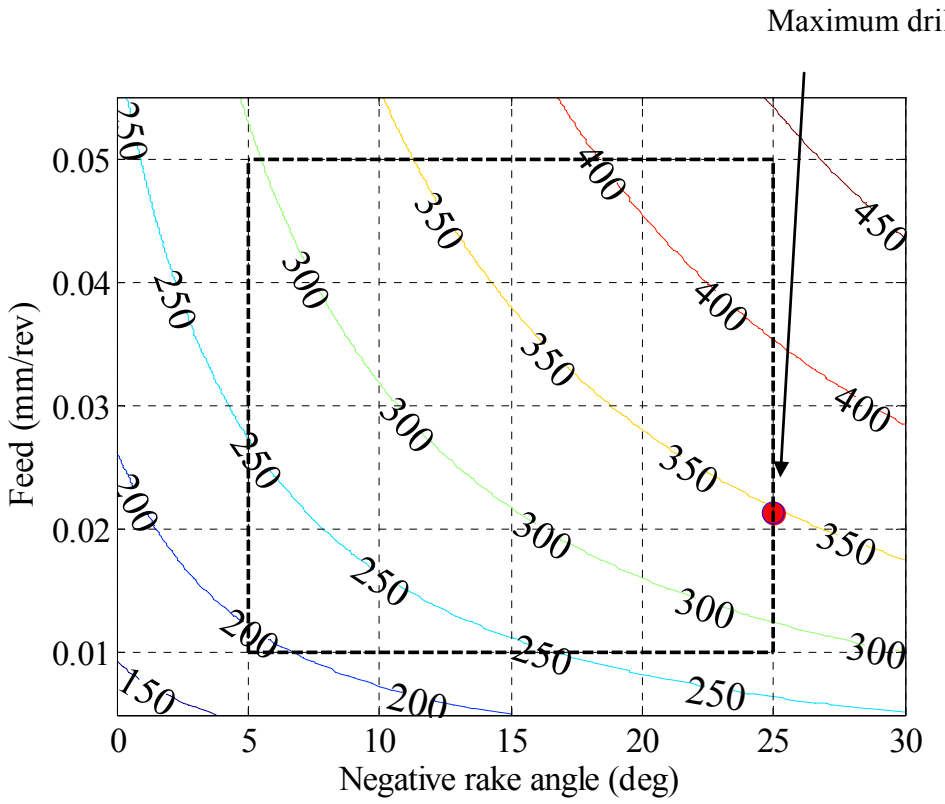

Figure 4.10: 2-D contour plot for rake angle & feed (YZ plane in slice plot)

Similarly, Figure 4.11 represents the 2-D representation of the tool-life response among rake angle and speed at optimum feed condition. In this plot, the optimum drilling depth

is indicated by blue dot which is the maximum rake angle and maximum speed in the selected conditions.

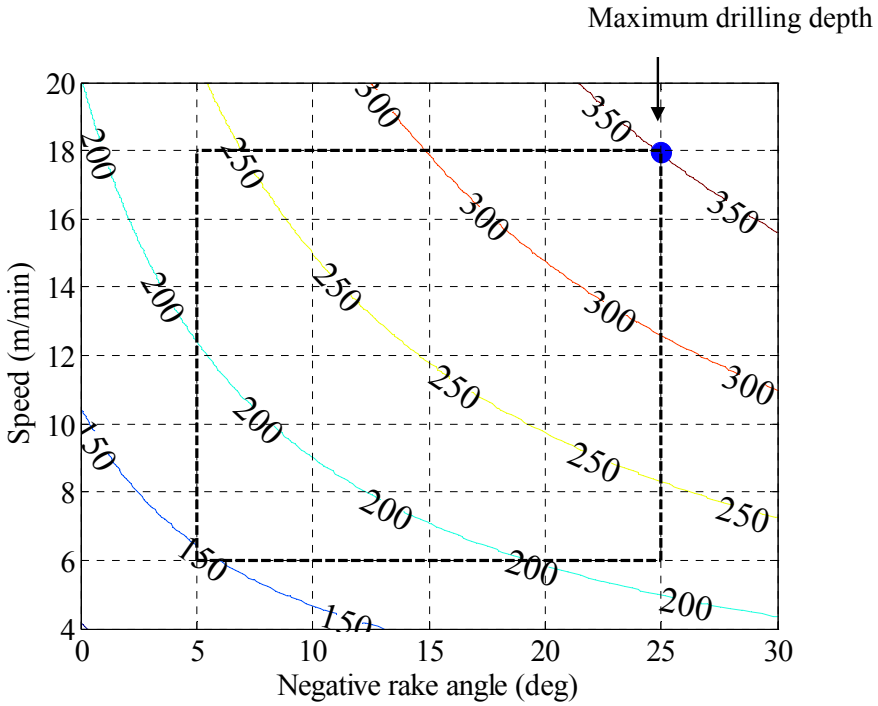

Figure 4.11: 2-D contour plot for rake angle & speed (XZ plane in slice plot)

The optimization results of the parameters in core drilling process for the constraints of drilling power 150 W, minimum thrust force 200 N, to obtain maximum drilling depth of 350 mm with intermittent drilling depth of 15 mm are therefore listed in Table 4.4.

Table 4.4: Optimization results for core drilling process on basalt rock

Parameter	**Selected range**	**Optimum values**
Cutting Speed	6 to 18 m/min	18 mm/min
Rotational Speed	60 to 180 rpm	180 rpm
Feed	0.01 to 0.05 mm/rev	0.021 mm/rev
Rake angle	-5° to -25°	-25°

In order to understand the impact of the selected constraints and flexibility provided by the optimization model, an arbitrary drilling power value of 100 W for similar minimum thrust force of 200 N are selected in the model and 2-D plot representing speed and feed is plot again as shown in Figure 4.12.

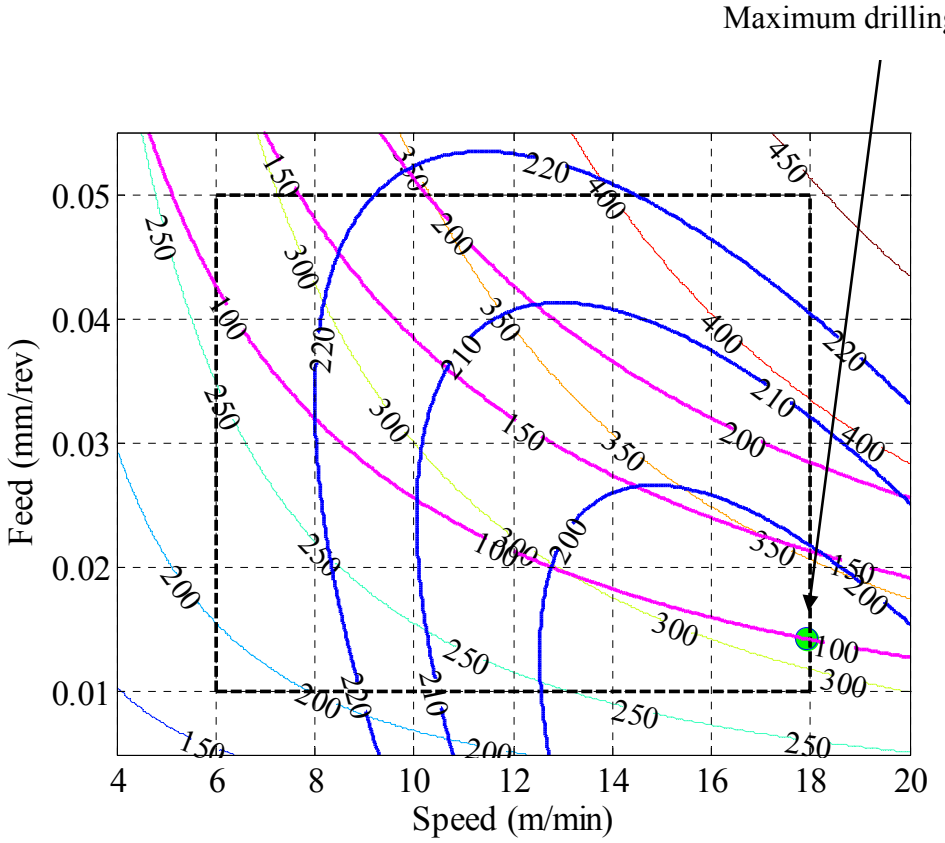

Figure 4.12: 2-D plot of speed Vs feed showing shift in optimization point when using less drilling power (100 W)

The maximum drilling depth predicted for the second set of constraints is 315 mm, with the optimum conditions as feed: 0.014 mm/rev, speed: 18 m/min and rake angle: -25°. Thus allowable drilling power plays an important role in determining the tool-life of the PCD compact core drill in basalt rock, restricting the maximum drilling depth and also

the optimum feed that can be used. Since optimum rotational speed is unchanged between the two scenarios, it can imply that rotational speed has less influence on tool-wear at higher values of drilling power than feed. If the available thrust force is less than 200 N, the drilling power has to be increased to obtain the maximum drilling depth because the core drill requires high speed conditions according to the optimization model.

CHAPTER 5

CONCLUSIONS AND FUTURE WORK

The current experimental investigation includes an optimization methodology for using PCD compact tools for dry core drilling of igneous rock, basalt. An empirical tool-wear model has been developed based upon the progressive tool-wear data for various cutting conditions and tool geometry. The parameters such as thrust force and torque have been measured and recorded during the experiments. They assisted in defining the constraints during optimization. The major conclusions that can be drawn from this thesis work are listed in the following section.

5.1 Conclusions

The summary of the experimental investigation presented in this research work are as follows.

1. The forces and torque required to drill basalt rock using core type drills have been measured for the experiments by varying the cutting conditions and rake angle of the PCD compact inserts for the incremental drilling depth of 15 mm.
2. An empirical tool-wear model has been developed to correlate the tool-life of PCD compact core drill in Martian simulant rock, basalt, for given set of cutting conditions and geometry. It is believed that the progressive tool-wear measurement for PCD compact core bit in the basalt rock is a novel approach in order to evaluate the drilling performance.

3. Based upon an optimization model, the maximum drilling depth of 350 mm (with intermittent drilling depth increments of 15 mm) can be achieved using PCD compact core drills in basalt rock under dry cutting conditions. The optimum rotational speed, feed and rake angle to achieve the above mentioned drilling depth are 180 rpm, 0.021 mm/rev and -25°, respectively.
4. The major technical constraints defining the drilling system that will be designed to collect the samples on Mars, namely minimum thrust force and drilling power have been integrated in the optimization methodology using the experimental data.
5. The influence of rock powder generated during the core drilling process has a profound effect on torque data. The dynamic vibrations generated by the core drill have also played a major role in the amount of fluctuation in thrust force and torque measurements. Also, a significant increase in the required thrust force is observed due to the rock powder at low-feed conditions.
6. The optimization of cutting conditions and geometry in igneous rock, basalt, would enable higher drilling depth in sedimentary rock formations that have been tested by other researchers. Until now, an optimization method has not been developed for Martian drilling applications.
7. It is noted that there is considerable variability of the strength of the basalt rock, which will need to be considered in future programs.

Future experiments can be carried out using the current optimum experimental conditions in Martian atmospheric pressures and temperatures to determine the tool-wear behavior

under such conditions. If the available minimum thrust force becomes greater than 200 N in Martian drilling, the optimum conditions are still valid, since drilling power influences the cutting conditions more than thrust force. On contrary, if the available thrust force is less than 200 N, the PCD compact core drill may not achieve optimum drilling depth with current conditions.

5.2 Suggestions for Future

This preliminary work will assist in the development of smart and sustainable drills for dry drilling applications for future missions on Mars planned by NASA.

This research work will establish a strong platform for developing quantitative relationships among drill materials, geometry, coatings, cutting conditions and drill wear for sustainable Martian dry drilling operations. The parameters chosen so far are cutting conditions and rake angle due to limitations on the design of tool. A new tool-design can be proposed reducing the diameter of the core drill and evaluating different geometries of PCD compact inserts. Drill bit design has been a criterion to evaluate the drilling performance in terrestrial drilling applications (Clayton et al., 2005).

Future experiments can be conducted under optimized conditions in Martian temperature and pressure in a vacuum chamber. An equipment to evacuate the rock powder while core drilling assists in determining the actual cutting forces thus providing accurate results for further analysis. The temperature of the core bit needs to be monitored during drilling, since tool-wear is temperature dependent phenomenon. The properties of the

basalt rock samples have been observed to be varying depending upon the location at which the samples are obtained, which needs to be addressed in future investigations.

Based on the experimental data, and using the analytical modeling methods and techniques, quantitative relationships can be established for the involved variables and measures of drilling performance such as thrust force and torque.

APPENDIX – I

Sample calculation of compressive strength of the basalt Rock 1 from the Equation 4.2 mentioned in chapter 4

For the cutting conditions, speed = 140 rpm, feed = 0.04 mm/rev and rake angle = -10° selected randomly from Table 4.1, the parameters measured after the experiments are given below.

1. Maximum thrust force = 402 N
2. Mean torque = 3.21 N-m
3. Average maximum flank wear = 0.063 mm
4. Length of the insert = 3.5 mm

Substituting the above values in Equation 4.2 below,

$$UCS = \left(\frac{Thrust\ \ force}{4 \times Flank\ wear \times length\ of\ \ the\ insert} \right) \quad \text{(Zacny and Cooper, 2007)}$$

$$\Rightarrow \qquad UCS = \left(\frac{402}{4 \times 0.063 \times 3.5} \right) \text{N/mm}^2 \qquad (\text{N/mm}^2 = \text{MPa})$$

$$\Rightarrow \qquad UCS = 456 \text{ MPa (Rock 1)}$$

Thus the compressive strength of Rock 1 can be determined with given thrust force value and flank wear measurement.

APPENDIX – II

Influence of tool natural vibrations on the torque measurements associated with length of the tool

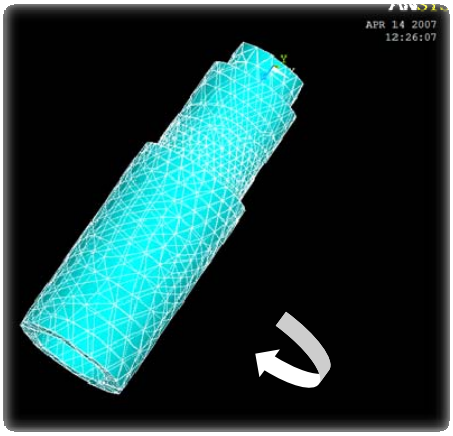

Initial tool length: 105 mm
Natural frequency - Torsion: 778 Hz

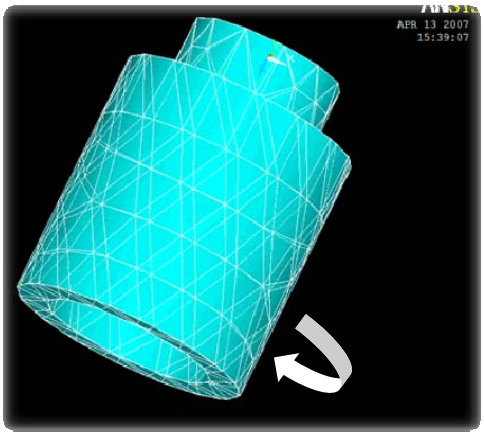

Current tool length: 54 mm
Natural frequency - Torsion: 1640 Hz

In earlier section 3.4.2, external vibrations were observed at 650 Hz in frequency domain shown in Figure 3.8, which are believed to be the influence of tool structure. By shortening the tool length from 105 mm to 54 mm the natural frequencies resonance related to torsion is increased to 1640 Hz, which is above the sampling frequency of 1000 Hz. Thus the influence of resonance in the measured data especially in the torque measurements can be avoided. The comparison of the torque measurements after reducing the tool length and increasing the sampling frequency accordingly are shown in Figure II.1.

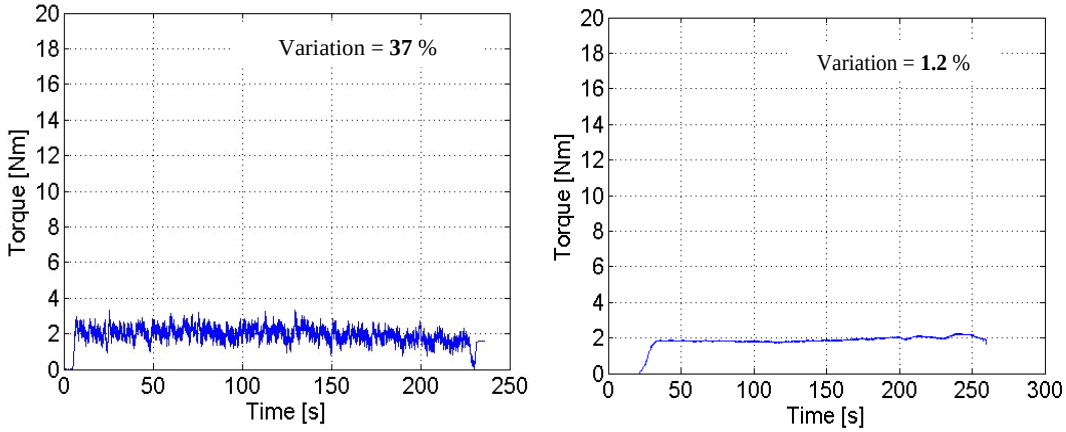

Figure II.1: Improvement in the torque measurements after reducing tool length and increasing sampling frequency from 10 Hz to 1000 Hz

(Speed: 140 rpm, Feed: 0.025 mm/rev, Drilling depth: 15 mm)

APPENDIX – III

Matlab (Version 7.1, R14) program for optimization of core drilling process in basalt rock sample using PCD compact core bit

The following program is used to find the results of optimization as shown in section 4.4. The coefficients determined by using multiple regression analysis are used to determine the maximum drilling depth mentioned in the objective function for range of speed, feed and rake angles. The maximum drilling depth is thus determined in the iterative loop by imposing the drilling power and minimum thrust force as constraints. The empirical equations for drilling power and minimum thrust force for the range of speed and feed conditions determine the contour plot representing constraints. Finally, the optimum conditions at which the drilling depth is maximum are displayed. The following program can be copied and run in a Matlab editor to obtain the optimization results and their corresponding plots.

```
% Start of the program
clear all
close all
clc
clf
% coefficients for prediction model of frank wear
C = 0.03639;
alpha1 = -0.17294;
beta1 = -0.10899;
sigh1 = -0.16488;
tita1 = 0.39464;
% upper limit for flank wear
Flankmax = 0.2;
V=linspace(6,18,300); % cutting speed 6-18 (m/min)
f=linspace(0.01,0.05,300); % feed 0.01-0.05 (mm/rev)
a=linspace(5,25,21); % rake angle 5 - 25 (deg)
V1=linspace(4,20,300); % cutting speed 6-18 (m/min)
f1=linspace(0.005,0.055,300); % feed 0.01-0.05 (mm/rev)
a1=linspace(5,25,21); % rake angle 5 - 25 (deg)
```

```
a2=linspace(0,30,21);
tstar = 0;
dstar = 0;
vstar = [];
fstar = [];
astar = [];
for i=1:300
   for j=1:300
      for k=1:21
         % calculate the number of hole based on the flank wear prediction model

Ddepth(i,j,k)=abs((Flankmax./(C.*V(i).^alpha1.*f(j).^beta1.*a(k).^sigh1)).^(1/tita1));

Ddepth1(i,j,k)=abs((Flankmax./(C.*V1(i).^alpha1.*f1(j).^beta1.*a1(k).^sigh1)).^(1/tita1)
);
         % calculate power and Thrust
         t(i,j,k)=(390.5*V(i)*f(j));
         t1(i,j,k)=(390.5*V1(i)*f1(j));

b1=422.9127;
b2=-2986.4;
b3=-27.2367;
b4=188.7755;
b5=19659;
b6=0.7813;
t2(i,j,k)=b1+b2*f(j)+b3*V(i)+b4*f(j)*V(i)+b5*(f(j))^2+b6*(V(i))^2;
         if ((t(i,j,k) <= 100) & (Ddepth(i,j,k) >= dstar))
            tstar = t(i,j,k);
            dstar = Ddepth(i,j,k);
            vstar = V(i);
            fstar = f(j);
            astar = a(k);
         end
      end
   end
end


fprintf('Maximum drilling depth : '),disp(dstar)
fprintf('Optimal speed : '),disp(vstar)
fprintf('Optimal feed : '),disp(fstar)
fprintf('Optimal rake angle : '),disp(astar)
fprintf('Constraint power : '),disp(tstar)

% show max Number of parts command window
% Ddepth_opt=max(max(max(Ddepth)))
```

```
% [Speed,Feed,Rakeangle] = meshgrid(6:1:18,0.01:0.001:0.05,5:1:25);
for i=1:300
for j=1:300
for k=1:21
if(Ddepth(i,j,k)==dstar)
row=i;column=j;page=k;
end
end
end
end
% show parameter coorespond to max number of parts
xslice = V(row);
yslice = f(column);
zslice = a(page);

figure(1)
slice(V1,f1,a2,Ddepth,xslice,yslice,zslice)
colormap jet
shading interp
colorbar
set(gca,'fontsize',12)
xlabel('Speed (m/min)','fontsize',12)
ylabel('Feed (mm/rev)','fontsize',12)
zlabel('Negative rake angle (deg)','fontsize',12)


figure(2)
[C,h]=contour(V1,f1,Ddepth1(:,:,page)');
hold
set(gca,'fontsize',14,'fontname','times')
clabel(C,h,'labelspacing',100,'fontsize',12,'fontname','times');
xlabel('Speed (m/min)','fontsize',14,'fontname','times');ylabel('Feed
(mm/rev)','fontsize',14,'fontname','times');
plot(vstar,fstar, 'marker','o','MarkerFaceColor','g','Markersize',10);
grid on;
l1=line([6,6],[.01,.05], 'linewidth',2);
set(l1,'color','black','linestyle','--');
l2=line([6,18],[.01,.01], 'linewidth',2);
set(l2,'color','black','linestyle','--');
l3=line([18,18],[.01,.05], 'linewidth',2);
set(l3,'color','black','linestyle','--');
l4=line([18,6],[.05,.05], 'linewidth',2);
set(l4,'color','black','linestyle','--');
hold on
[Ct,ht]=contour(V1,f1,t1(:,:,page)',[100, 150, 200],'m-');
```

```
set(ht,'linewidth',2,'linestyle','--');
clabel(Ct,ht,'labelspacing',200,'fontsize',12,'fontname','times');
[Ct2,ht2]=contour(V1,f1,t2(:,:,page)',[200 210 220],'m-');
set(ht2,'color','blue', 'linewidth',2,'linestyle','-');
clabel(Ct2,ht2,'labelspacing',200,'fontsize',12,'fontname','times');
% colorbar('vert')
hold off

for i=1:300
   for j=1:21
   m(i,j)=Ddepth1(row,i,j)';
   n(i,j)=Ddepth1(i,column,j)';
   n1(i,j)=Ddepth1(i,column+40,j)';
   end
end



figure(3)
[C1,h1]=contour(a2,f1,m);
hold
set(gca,'fontsize',14,'fontname','times')
clabel(C1,h1,'labelspacing',100,'fontsize',16,'fontname','times');
xlabel('Negative rake angle (deg)','fontsize',14,'fontname','times');ylabel('Feed
(mm/rev)','fontsize',14,'fontname','times');
plot(astar,fstar, 'marker','o','MarkerFaceColor','r','Markersize',10);
grid on;
l1=line([5,5],[.01,.05], 'linewidth',2);
set(l1,'color','black','linestyle','--');
l2=line([5,25],[.01,.01], 'linewidth',2);
set(l2,'color','black','linestyle','--');
l3=line([25,25],[.01,.05], 'linewidth',2);
set(l3,'color','black','linestyle','--');
l4=line([25,5],[.05,.05], 'linewidth',2);
set(l4,'color','black','linestyle','--');


figure(4)
[C2,h2]=contour(a2,V1,n1);
set(gca,'fontsize',14,'fontname','times')
hold
clabel(C2,h2,'labelspacing',100,'fontsize',16,'fontname','times');
xlabel('Negative rake angle (deg)','fontsize',14,'fontname','times');ylabel('Speed
(m/min)','fontsize',14,'fontname','times');
plot(astar,vstar, 'marker','o','MarkerFaceColor','b','Markersize',10);
grid on;
```

```
l1=line([5,5],[6,18], 'linewidth',2);
set(l1,'color','black','linestyle','--');
l2=line([5,25],[6,6], 'linewidth',2);
set(l2,'color','black','linestyle','--');
l3=line([25,25],[6,18], 'linewidth',2);
set(l3,'color','black','linestyle','--');
l4=line([25,5],[18,18], 'linewidth',2);
set(l4,'color','black','linestyle','--');
% colorbar('vert')

% End of program
```

APPENDIX – IV

Sample calculations using empirical equations developed for drilling power and minimum thrust force in section 4.1.3.

a) The empirical equation for drilling power is given below,

$$Drilling\ power = a0 + a1 \times speed \times feed$$

where $a0 = 0.01985$, $a1 = 39.05$.

For *speed* = 180 rpm and *feed* = 0.02 mm/rev, *Drilling power* = 141 W.

b) The minimum thrust force can be determined for given speed and feed by using following quadratic equation,

$$Minimum\ thrust\ force = b0 + b1 \times feed + b2 \times speed + b3 \times speed \times feed + b4 \times feed^{2} + b5 \times speed^{2}$$

where $b0 = 422.9127$; $b1 = -2986.4$; $b2 = -2.7237$; $b3 = 18.8776$; $b4 = 19659$; $b5 = 0.00781$.

For *speed* = 180 rpm and *feed* = 0.02 mm/rev, *Minimum thrust force* = 194 N

REFERENCE

"Evaluating the Biological Potential in Samples Returned from Planetary Satellites and Small Solar System Bodies", http://www7.nationalacademies.org/ssb/sssbapd.html Planetary Protection Policy, as accessed on 10/19/2007.

Alauddin M. and El Baradie M.A., "Tool Life Model for End Milling Steel (190 BHN)", *Journal of Materials Processing Technology*, Vol. 68, 1997, pp. 50 - 59.

Anttila M., Suomela J. and Saarinen J., "The Micro Rosa2 Activity - Conclusion and Future Plans", *7th ESA Workshop on Advanced Space Technologies for Robotics and Automation ASTRA*, The Netherlands, 2002, pp. 19-21.

Anttila M. and Ylikorpi T., "Defining the Technical Requirements for Subsurface Mars Drilling", *Sixth International Conference on Mars*, 2003, Paper 3020.

Appl F.C., Wilson C.C. and Lakshman I., "Measurement of Forces, Temperature and Wear of PDC Cutters in Rock Cutting", *Wear*, Vol. 169, 1993, pp. 9 - 24.

Bar-Cohen Y., Bao X., et al., "An Ultrasonic Sampler and Sensor Platform for In-situ Astrobiological Exploration", *Proceedings of the SPIE Smart Structures Conference*, San Diego, CA, USA, 2003.

Checkina O.G., Goryacheva I.G. and Krasnik V.G., "The Model for Tool Wear in Rock Cutting", *Wear*, Vol. 198, 1996, pp. 33 - 38.

Clayton R., Chen S. and Lefort G., "New Bit Design, Cutter Technology Extend PDC Applications to Hard Rock Drilling", *Journal of Petroleum Technology*, Vol. 27, 2005, pp 63-64.

Davim J.P. and Antonio C.A.C., "Optimal Drilling of Particulate Metal Matrix Composites based on Experimental and Numerical Procedures", *International Journal of Machine Tools & Manufacture*, Vol. 41, 2001, pp. 21 - 31.

Ersoy A. and Waller M.D., "Drilling Detritus and the Operating Parameters of Thermally Stable PDC Core Bits", *International Journal of Rock Mechanics and Mining Sciences*, Vol. 34 (7), 1997, pp. 1109 - 1123.

Finzi A.E., Lavagna M. and Rocchitelli G., "A Drill-soil System Modelization for Future Mars Exploration", *Planetary and Space Science*, Vol. 52, 2004, pp. 83 - 89.

Glindermann G., Edwards M. and Morgenstern P., "Phosphine from Rocks: Mechanically Driven Phosphate Reduction?" *Environmental Science Technology*, Vol. 39, 2005, pp. 8295 - 8299.

Glowka D.A., "Implications of Thermal Wear Phenomena for PDC Bit Design and Operation", Sandia National Laboratories, 1985.

Grady D.E., "Spall Properties of Solenhofen Limestone and Dresser Basalt", *Shock Compression of Condensed Matter*, 1999, pp. 1255 - 1258.

Ilio D. A. and Togna A., "A Theoretical Wear Model for Diamond Tools in Stone Cutting", *International Journal of Machine Tools & Manufacture*, Vol. 43, 2003, pp. 1171 - 1177.

Jawahir I.S. and Wang X., "Development of Hybrid Predictive Models and Optimization Techniques for Machining Operations", *Journal of Materials Processing Technology*, Vol. 185, 2007, pp. 46- 59.

Kolle J.J., "The Effects of Pressure and Rotary Speed on the Drag Bit Drilling Strength of Deep Formations", *Society of Petroleum Engineers*, Denver, Colorado, USA, 1996, SPE 36434.

Lee B.Y., Lui H.S. and Tarng Y.S., "Modeling and Optimization of Drilling Process", *Journal of Materials Processing Technology*, Vol. 74 (1 - 3), 1998, pp. 149 - 157.

Lei S. and Kaitkay P., "Micromechanical Modeling of Rock Cutting under Pressure Boundary Pressure Boundary Conditions using Distinct Element Method", *NAMRI/SME*, 2002, pp. 207 - 214

Lin T., Hood M., et al., "Wear and Failure Mechanisms of Polycrystalline Diamond Compact Bits", *Wear*, Vol. 156, 1992, pp. 133 - 150.

Magnani P.G., Re E., et al., "Deep drill (DeeDri) for Mars Application", *Planetary and Space Science*, Vol. 52, 2004, pp. 79 - 82.

Rao K.U.M. and Misra B., "Wear of Diamond Grits of Diamond Core Drills", *Indian Journal of Engineering & Materials Sciences*, Vol. 2, 1995, pp. 18 - 23.

Sheldon G.L., "Forming Fibers from Basalt Rock", *Platinum Metals Rev.*, Vol. 21 (1), 1977, pp. 18 - 24.

Spencer R.L., "Introduction to Matlab", 2000.

Stavropoulou M., "Modeling of Small-diameter Rotary Drilling Tests on Marbles", *International Journal of Rock Mechanics and Mining Sciences*, Vol. 43, 2006, pp. 1034 - 1051.

Wang X. and Jawahir I.S., "Optimization of Multi-pass Turning Operations using Genetic Algorithms for the Selection of Cutting Conditions and Cutting Tools with Tool-wear

effect", *International Journal of Production Research*, Vol. 43 (17), 2002, pp. 3543 - 3559.

Wang X. and Jawahir I.S., "Web-based Optimization of Milling Operations for the Selection of Cutting Conditions using Genetic Algorithms", *Journal of Engineering Manufacture*, 2004, pp. 647 - 655.

Wanigarathne P.C., Kardekar A.D., et al., "Progressive Tool-wear in Machining with Coated Grooved Tools and its Correlation with Cutting Temperature", *Wear*, Vol. 259, 2005, pp. 1215 - 1224.

Wilson C. and Vorono O.A., "Diamond Turning of Granite", *Key Engineering Materials*, Vol. 250, 2003, pp. 138 - 146.

Wise J.L., Grossman J.W., et al., "Latest Results of Parameter Studies on PDC Drag Cutters for Hard-Rock Drilling", *Geothermal Resources Council Transactions*, Vol. 29, 2005, pp. 545 - 552.

Wyatt M.B. and McSween Jr.H.Y., "Spectral Evidence for Weathered Basalt as an Alternative to Andesite in the Northern Lowlands on Mars", *Nature*, Vol. 417, pp. 263 - 266.

Zacny K., Glaser D., et al., "Drilling Results in Ice-bound Simulated Lunar Regolith (FJS-1) as Part of the Construction and Resource Utilization Explorer Project (CRUX)", *Lunar and Planetary Science*, Vol. XXXVII, 2006.

Zacny K.A. and Cooper G.A., "Evaluation of a New Thermally Stable Polycrystalline Diamond Material in Soft and Hard Formations", *ASME Engineering Technology Conference on Energy*, Houston, TX, 2002, pp. 325 - 333.

Zacny K.A. and Cooper G.A., "Investigation of Diamond-impregnated Drill Bit Wear while Drilling under Earth and Mars Conditions", *Journal of Geophysical Research*, Vol. 109, 2004.

Zacny K.A. and Cooper G.A., "Laboratory Drilling under Martian Conditions yields Unexpected Results", *Journal of Geophysical Research*, Vol. 109, 2004.

Zacny K.A. and Cooper G.A., "Investigation of the Performance of a Coring Bit in Frozen Mud under Martian Conditions of Low Temperature and Pressure", *Journal of Geophysical Research*, Vol. 110, 2005.

Zacny K.A. and Cooper G.A., "Strategies for Drilling on Mars", *American Geophysical Union*, 2005.

Zacny K.A. and Cooper G.A., "Considerations, Constraints and Strategies for Drilling on Mars", *Planetary and Space Science*, Vol. 54, 2006, pp. 345 - 356.

Zacny K.A. and Cooper G.A., "Coring Basalt under Mars Low Pressure Conditions", *The International Journal of Mars Science and Exploration*, Vol. 3, 2007, pp. 1 - 11.

Zacny K.A., Cooper G.A. and Quayle M.C., "Enhancing Cuttings Removal with Gas Blasts while Drilling on Mars", *Journal of Geophysical Research*, Vol. 110, 2005.

VITA

The author was born in Hyderabad, India on March 5, 1981. He finished his Bachelor of Engineering in Mechanical Engineering with specialization in production engineering from Osmania University, Hyderabad, India in 2004. He pursued a Master's degree in Manufacturing Systems Engineering at the University of Kentucky, Lexington, USA. During his graduate study, he worked as a research assistant for the Machining Research Laboratory at the Center for Manufacturing in the university.

Sandeep Manthri

Date: 11/06/2007